Chapter 9
Plasma-Catalytic Conversion of Carbon Dioxide

Bryony Ashford, Yaolin Wang, Li Wang, and Xin Tu

9.1 Introduction

The emission of CO_2 is a pressing concern as its release into the atmosphere is a major source of global warming. As global temperatures rise due to the greenhouse effect and current technologies, such as carbon capture and storage (CCS) and a switch to renewables, fall short, expertise must be employed to find new, viable processes for the mitigation of CO_2. Focus is now on carbon dioxide utilization, as high-value chemicals and fuels can be produced, creating viable and sustainable processes. Current processes, however, such as thermal catalytic and electrochemical processes, require elevated temperatures and are not thermodynamically efficient, thus reducing their energy efficiency and feasibility. Plasma-catalytic processes have the potential to overcome these drawbacks due to their low-temperature operation and non-equilibrium characteristics which allow the high stability of the CO_2 molecule to be overcome without the need for large energy inputs. Alongside this, the catalyst acts to lower the activation barrier and enhance the selectivity to the required product. Interactions also occur between the catalyst and the plasma, creating synergy. Furthermore, quick start-up and shutdown enable plasma-catalytic processes to be used as a method of storing excess energy from renewable energy generation. A great number of reactions can potentially be carried

B. Ashford · Y. Wang · X. Tu (✉)
Department of Electrical Engineering and Electronics, University of Liverpool, Liverpool, UK
e-mail: xin.tu@liverpool.ac.uk

L. Wang
State Key Laboratory of Fine Chemicals, School of Chemical Engineering, Dalian University of Technology, Dalian, Liaoning, China

College of Environmental Sciences and Engineering, Dalian Maritime University, Dalian, Liaoning, China

Department of Electrical Engineering and Electronics, University of Liverpool, Liverpool, UK

X. Tu et al. (eds.), *Plasma Catalysis*, Springer Series on Atomic, Optical, and Plasma Physics 106, https://doi.org/10.1007/978-3-030-05189-1_9

out in a plasma-catalytic reactor, including CO_2 decomposition, dry reforming of methane and CO_2 hydrogenation; hence a great number of high-value products can be created (oxygenates, liquid hydrocarbons, syngas, etc.). Currently, a trade-off exists between high energy efficiency and high reactant conversion. This is due to conversion increasing with input power, which leads to a decrease in energy efficiency. A greater understanding of the plasma chemistry and the interactions between plasma and catalyst will further increase the viability of plasma-catalytic processes for the utilization of CO_2 on an industrial scale. The following chapter describes this process in detail for a number of different reactions and discusses recent advances in the area.

9.1.1 Carbon Dioxide Emission

Carbon dioxide is a major greenhouse gas and is largely responsible for the changes we are currently seeing in the climate. Since the industrial revolution, greenhouse gas emissions have risen, with a 75% global increase in greenhouse gases occurring since 1970. In 2010, 49×10^9 tonnes of CO_2 equivalent ($GtCO_2eq$) of greenhouse gases were emitted from anthropogenic sources, of which CO_2 sources currently make up the majority at 76% [1]. Industrial development and the release of carbon dioxide have always gone hand in hand, and with many countries still developing their industry and a rising global population, carbon dioxide emissions will continue to increase. As is well documented, a rise in CO_2 in the atmosphere leads to warming of the planet, causing a rise in sea level which can wipe out whole communities in low-lying areas and increasing the frequency of disasters such as tsunamis and forest fires. In recent years, these disasters have become more commonplace, resulting in societal values changing to reflect the growing urgency of the situation and forcing governments around the world to take action against climate change. This need for change culminated in the Paris Agreement, a legally binding document between 195 countries that aims to tackle climate change, aiming to limit the global temperature rise to well below 2 °C above pre-industrial levels. In order to fulfill targets set out in the agreement, a switch to renewable energy and a reduction in the release of greenhouse gases into the atmosphere are required, necessitating the design of novel technologies that enable this change while allowing society to prosper. The utilization of carbon dioxide from waste gas streams is one area which has the potential to fulfill these requirements, as CO_2 from fossil fuel and industrial processes accounts for 65% of total annual anthropogenic greenhouse gas emissions, as detailed in the Fifth Assessment Report of Intergovernmental Panel on Climate Change (IPCC) [1]. A significant reduction in carbon dioxide emissions can therefore be made by capturing CO_2 from waste gas streams and converting it into valuable fuels and chemicals.

9.1.2 Current Technologies to Reduce CO_2 Emission

There are several methods that can be used to convert carbon dioxide, including catalytic conversion, photocatalytic/photochemical processes, electrocatalytic/electrochemical processes, enzymatic/biochemical processes and plasma processes. Each of these methods results in a slight variation in the product created, with hydrocarbons, hydrogen and oxygenates forming via catalytic conversion, while carbon monoxide, hydrocarbons, syngas and oxygenates are the main products of plasma processes. Along with the need for high temperatures in thermal-catalytic processes, issues can be encountered with catalyst deactivation due to coking. Electrocatalytic processes show promise for producing methanol, formic acid and a variety of other organic chemicals. However, these processes have low thermodynamic efficiency. The least researched, yet predicted to be the most effective, is the plasma process [2, 3]. In comparison to the other processes, it is simple and fast: plasma has the potential to enable thermodynamically unfavorable chemical reactions (e.g. CO_2 dissociation) to occur at ambient conditions [3].

9.1.3 Carbon Dioxide Utilization Through Plasma Technology

Nonthermal plasma (NTP) can be operated at room temperature and atmospheric pressure while still generating highly active species and electrons, with mean electron energy between 1 and 10 eV. This electron energy is the optimum range for exciting molecular and atomic species and breaking chemical bonds. For CO_2 dissociation (9.R1) to occur in plasma, only 5.5 eV is required to break the OC = O bond via stepwise vibrational excitation. Nonthermal plasma therefore shows great potential in the production of an efficient CO_2 utilization process, as it can overcome the stability of CO_2 without the need for the high temperatures required in thermal catalytic processes. Plasma technology is also advantageous over thermal processes as reaction rates are high and steady state is quickly reached [4]. This facilitates quick start-up and shutdown, a promising feature that enables plasma technology powered by renewable energy to act as efficient chemical energy storage through a localized or distributed system at peak grid times [5]. Different routes for CO_2 conversion have been explored using NTP (Fig. 9.1).

9.2 Plasma CO_2 Decomposition

$$2CO_2 \rightarrow 2CO + O_2 \qquad (9.R1)$$

Decomposition of CO_2 into CO and O_2 using NTP has recently attracted significant interest as this reaction is almost impossible at low temperatures using

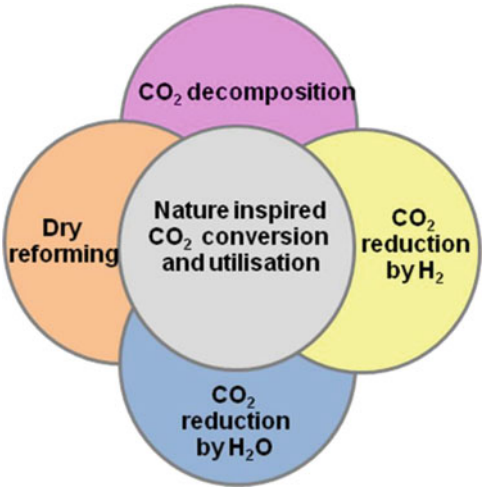

Fig. 9.1 Different routes for CO_2 conversion

conventional catalysis. Furthermore, the product CO is an important chemical feedstock for further synthesis of fuels and chemicals. Various plasma systems are reported to successfully convert CO_2 into CO and O_2 (9.R1), including glow discharge, where one study found a CO_2 conversion of 30% is achievable at an input voltage of 7 kV [6]; radio frequency discharge, which can achieve 90% CO_2 conversion at 1 kW [7]; and microwave discharge, in which a 100 W power input was accompanied by a 90% conversion [8]. A carrier gas, such as helium or argon, has previously been commonplace in the dissociation of CO_2 via plasma systems; however, this leads to an additional, undesired cost. Dielectric barrier discharge (DBD) reactors have been shown to successfully dissociate CO_2 in the absence of a carrier gas [9, 10], with one study achieving 30% conversion at a power density of 14.75 W/cm^3 [10].

In plasma, reactions mainly occur in the gas phase. Firstly, CO_2 is dissociated into CO and an oxygen atom. The oxygen atom created then either combines with another oxygen atom to form molecular oxygen (9.R2), or it reacts with CO_2 to form carbon monoxide and an oxygen molecule (9.R3):

$$O + O \rightarrow O_2 \tag{9.R2}$$

$$O + CO_2 \rightarrow O_2 + CO \tag{9.R3}$$

The production of carbon can also occur (9.R4), along with reverse CO_2 decomposition (9.R5):

$$CO + e \rightarrow C + O + e \tag{9.R4}$$

$$CO + O \rightarrow CO_2 \tag{9.R5}$$

CO_2 conversion mainly occurs via electronic dissociation, vibrational excitation and dissociative attachment [11]. A zero-dimensional chemical kinetics model has

been developed to understand the reaction mechanisms in the plasma CO_2 dissociation [12]. Electron impact dissociation has been found dominant in CO_2 decomposition in DBD plasmas, leading to lower energy efficiency compared to microwave plasmas or gliding arc discharges, in which more energy-efficient vibrational excitation of CO_2 plays a key role in the decomposition of CO_2 [13–15]. A 1D model developed for an AC gliding arc reactor has shown that dissociation only occurs at the center of the arc where the gas, vibrational and electron temperatures, as well as the ionization degree, are at their maximums [13]. The dissociation of CO_2 in a gliding arc therefore only occurs significantly at the arc center. In a typical microwave plasma, gas temperature has shown to be an important factor in determining CO_2 conversion, with a higher temperature resulting in a greater conversion; as temperature increases, the reaction rate coefficients for heavy-particle dissociation also increase, along with the number of vibrationally excited species [16].

The reformation of CO_2 can be an issue in plasma reactors, decreasing the effective CO_2 conversion as CO recombines with oxygen species (O_2, O and O^{2-}) [17]. A novel approach to solving this problem was carried out by Mori and Tun, in which a DBD reactor was combined with a solid oxide electrolyser cell (SOEC) [17]. The SOEC was used to remove oxygen from the gas, hence restricting it from reacting with CO. The SOEC also contributed to CO_2 splitting [17]. When the two were used separately for this reaction, the SOEC process reached a maximum conversion of 3%, while the plasma-alone process had an optimum conversion of 15%. However, when combined, a synergistic effect occurred as the hybrid system reached a conversion of 93%, which was attributed to the SOEC removing oxygen from the system, as shown in Fig. 9.2 [17]. It is novel ideas such as this which can greatly increase the feasibility of plasma CO_2 decomposition on an industrial scale.

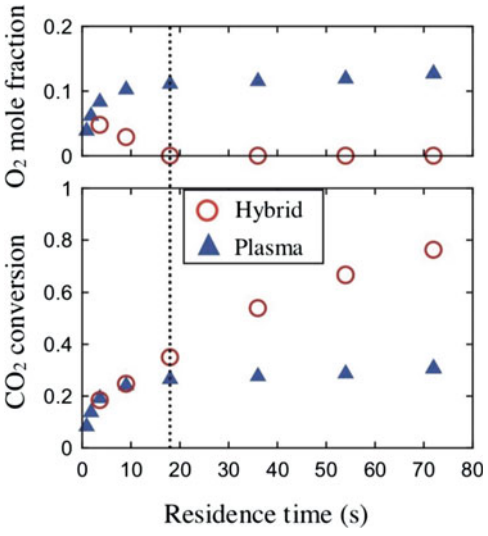

Fig. 9.2 CO_2 conversion and outlet O_2 mole fraction with residence time (plasma input power, 30 W; SOEC applied voltage, 7 V; SOEC current, 37–50 mA; CO_2 flow rate, 0.23–18 ml/min; pressure, 3 kPa; inside heater temperature, 800 °C; outside furnace temperature, 200 °C) [17]

9.2.1 *Influence of Process Parameters*

A design of experiments approach using a cylindrical DBD revealed that the main parameter which affects the energy efficiency of this process is the feed flow rate, while discharge power has the greatest influence on CO_2 conversion [18]. A high feed flow rate leads to a lower CO_2 conversion but is more energy efficient [18]. A high feed flow rate corresponds to a lower residence time, resulting in fewer interactions between the feed gases and the excited species, hence a lower conversion; however, a higher flow rate leads to lower specific energy input (SEI) (at constant plasma power) (Eqs. 9.1 and 9.2) and thus results in a more energy-efficient process (Eq. 9.3) (equations found in [19]) [12]:

$$\text{SEI}\,[\text{kJ/L}] = \left(\frac{\text{Power}\,[\text{kW}]}{\text{Flow}\,[\text{L/ min}]}\right) \times 60\,[\text{s/ min}] \tag{9.1}$$

$$\text{Power} = (1/T)\int_0^T (V(t) \times I(t))dt \tag{9.2}$$

$$E[\%] = \frac{\Delta H_r[\text{kJ/mol}] \times X_{CO_2}[\%]}{\text{SEI}[\text{kJ/L}] \times \text{molar volume}[\text{L/mol}]} \tag{9.3}$$

A trade-off therefore exists between energy efficiency and conversion, as energy efficiency decreases with increasing SEI, but conversion rises [12]. However, although SEI can remain constant when varying both plasma power and residence time simultaneously, a constant SEI does not necessarily result in the same values of CO_2 conversion and energy efficiency. In fact, it has been found that obtaining the same value of SEI using varying combinations of residence time and plasma power can lead to changes in reaction performance [12]. At high residence time and low plasma power, the maximum CO_2 conversion reached can be greater than when a low residence time and high power, but the same SEI, are used [12]. The effect of residence time on the conversion and energy efficiency is therefore greater than the effect of the plasma power. This is due to the length of time CO_2 stays within streamers (longer for a high residence time) being the major influencing factor on conversion, as opposed to high streamer intensity (as a result of high plasma power). At high SEIs, energy efficiency and conversion can therefore be increased simultaneously; however, energy efficiencies will be low even when maximized [12].

Discharge gap can play an important role in determining CO_2 conversion and energy efficiency. At constant SEI, an increase in discharge gap can lead to a decrease in energy efficiency and conversion if the increase is large enough to alter the streamer behavior [12, 20]. Smaller discharge gaps allow more streamers with higher peak currents to form; therefore, an increase in CO_2 dissociation occurs due to the greater effective plasma volume, while the increase in electron density resulting from the higher peak currents leads to a rise in electron impact reaction rates [12]. Alongside this, the average electron energy will be larger for smaller gaps; hence when collisions occur, more energy will be transferred [12].

The influence of discharge length has also been evaluated, with results showing that an increase in both discharge length and discharge power leads to an increased CO_2 conversion [20, 21]. This is due to higher discharge power resulting in an increase in the number of micro-discharges, thereby increasing the number of reaction channels for collisions to occur [20, 22]. However, this only appears to be the case up to a certain point, with one study finding an increase in applied power above 80 W results in a decreased conversion, possibly due to a change in discharge mode from surface discharge to filamentary discharge [19].

Dielectric material and frequency have been found to have no influence on the energy efficiency and CO_2 conversion [12, 20]. Alumina and quartz dielectrics were compared at various SEI values with results showing no significant differences in reaction performance between the two [12]. By contrast, Mei and Tu al reported that the thickness of dielectric materials affects the plasma conversion of CO_2 and energy efficiency using a DBD reactor [20]. Increasing the thickness of a quartz tube from 1.5 to 2.5 mm decreased the CO_2 conversion and energy efficiency of the plasma process by around 15% at a SEI of 120 kJ/L and a constant discharge gap of 2.5 mm [20]. In addition, they found that using a screw-type inner electrode in the DBD reactor significantly enhanced the conversion of CO_2 and energy efficiency compared to the reaction using a rod electrode [20]. The sharp edge of the screw-type electrode could distort the electric field and enhance the local electric field around the inner electrode and consequently generate more intensified filamentary discharge which can also be evidenced by increased amplitude and number of current pulses. This effect could generate more reaction channels for CO_2 conversion and makes a contribution to the enhanced reaction performance [20] (Fig. 9.3).

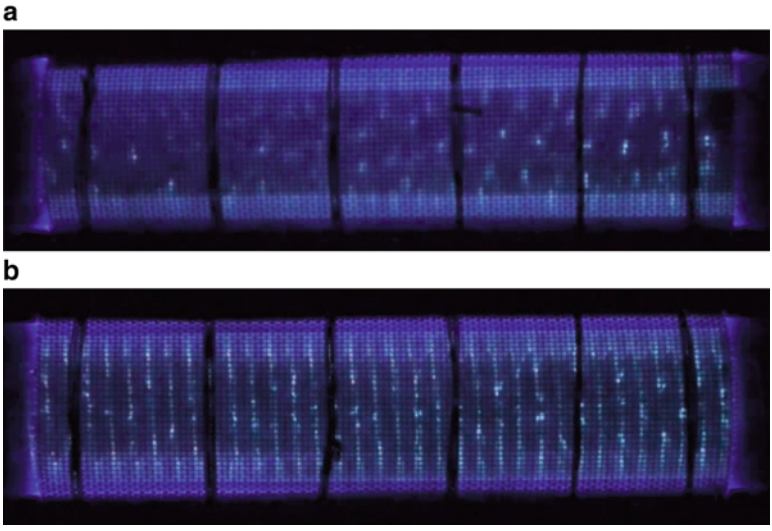

Fig. 9.3 Images of the CO_2 DBD plasma: (**a**) rod inner electrode; (**b**) screw-type inner electrode (discharge power, 40 W; discharge gap, 2.5 mm; discharge length, 100 mm; CO_2 feed flow rate, 25 mL/min; frequency, 9 kHz; outer electrode, stainless steel mesh) [20]

A diluent gas, such as helium or argon, can be used in the feed alongside CO_2. The addition of such gases can lead to a higher absolute CO_2 conversion in a DBD; however, if total feed rate is kept constant, the actual amount of CO_2 converted (effective CO_2 conversion) will be lower in the mixed feed (CO_2 + diluent) than for a pure CO_2 feed due to the decrease in CO_2 present in the feed [23]. The increase in absolute CO_2 conversion in the diluted feed can be explained by the lower breakdown voltage and the increased plasma formation due to an increase in plasma capacity; the addition of helium causes a more homogeneous plasma to form, while argon results in a greater micro discharge filament density [23]. As the threshold energies for inelastic collisions involving He and Ar are much higher than those for CO_2, and electron recombination is favored for CO_2^+ ions over Ar^+ and He^+, a greater fraction of plasma power will go into dissociating CO_2 and less will go into gas breakdown as this can occur at a lower voltage due to an increase in the electron mean free path [23]. As well as increasing conversion, this also leads to an increase in energy efficiency. However, as a large fraction of the input energy goes into exciting the diluent gas, the effective energy efficiency drops in comparison to the pure CO_2 feed [23].

A different effect results when N_2, an impurity present in many waste gas streams, is added to the pure CO_2 feed in DBD plasma. Below 50% N_2, the absolute CO_2 conversion increases as N_2 molecules enhance conversion due to the collision between N_2 metastable molecules and CO_2 resulting in CO_2 dissociation; thus, the effective conversion is tantamount to that of pure CO_2 as the increase in absolute CO_2 conversion cancels out the decrease in CO_2 in the feed [24]. However, above 50% N_2, a greater fraction of the input energy is transferred to N_2 molecules rather than going into CO_2 dissociation; hence effective CO_2 conversion and energy efficiency decrease [24]. The effect of N_2 addition to the feed differs in microwave plasma. Here, the effect on CO_2 conversion and energy efficiency is similar to that found when Ar or He is added to the feed in DBD plasma: absolute CO_2 conversion increases in comparison to pure CO_2 feed; however the reduction in CO_2 concentration results in a lower effective conversion and energy efficiency [25]. Absolute CO_2 conversion increases with a rise in N_2 concentration due to partial conversion of lower CO_2 vibrational levels into higher ones [25]. An important point to note is that on addition of N_2 at all concentrations to both microwave and DBD systems, harmful gases such as N_2O and NO_x are formed [24, 25].

9.2.2 Influence of Packing and Catalytic Materials

In current plasma systems, a trade-off exists between CO_2 conversion and energy efficiency [7, 26]. In order to solve this problem and hence create a feasible industrial process, further modification of the plasma system is required. One such modification is the addition of a catalyst into the plasma discharge, as research shows the hybrid plasma-catalytic process can result in higher CO_2 conversion while maintaining low energy consumption [19, 27]. The combination of plasma and

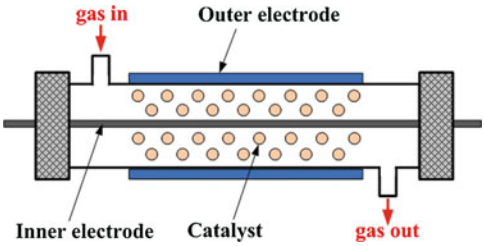

Fig. 9.4 Single-stage setup in a plasma-catalytic DBD reactor

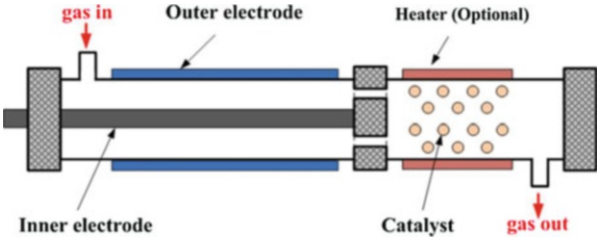

Fig. 9.5 Two stage setup in a plasma-catalytic DBD reactor

catalyst allows the beneficial aspects of each to be realized, along with the effect resulting from their interaction [28, 29]. This can lead to synergy in relation to conversion and efficiency, thus creating a more feasible process for the utilization of CO_2 on an industrial scale. When a catalyst is combined with plasma, the reactions that occur change from purely gas phase to a mixture of gaseous and heterogeneous [11]. The simplest method of combining plasma and catalyst in a single-stage setup is to do so in a DBD reactor (Fig. 9.4), as the catalyst can be placed directly into the discharge without the need for any adjustments in reactor geometry. In this setup, the catalyst is in direct contact with the plasma and can therefore interact with short-lived active species such as excited-state atoms and molecules, reactive radicals, photons and electrons.

In the two-stage setup (Fig. 9.5), a catalyst is placed downstream of the plasma discharge. The catalyst is not in direct contact with the plasma; hence it cannot interact with short-lived excited species, only with the exit gas which contains long-lived intermediates and, possibly, vibrationally excited species.

Catalysts can be incorporated into DBD reactors in a fully or partially packed-bed configuration [30, 31]. By mixing the catalyst and cheap packing material (e.g. glass beads, Al_2O_3 and quartz wool) before placing in the reactor, a packed-bed effect can also be realized without the need for high volumes of costly catalyst in addition to a catalytic effect. This setup also results in a quasi-homogeneous dispersion of the catalyst, which benefits the reaction performance as a greater number of CO_2 molecules will come into contact with the catalyst. The packing material can also lead to an increase in both CO_2 conversion and energy efficiency simultaneously. Zirconia beads with diameters in the range of 1.6–1.8 mm have been shown to increase CO_2 conversion by almost 100% while nearly doubling the energy efficiency in comparison to values obtained in the absence of any packing material [19].

The presence of a packing material will decrease the residence time of CO_2 molecules in the plasma when a fully packed bed is used. As mentioned in Sect.

9.2.2 on the effect of various process parameters, a decreased residence time results in a decrease in CO_2 conversion as there is less time for the feed gases and excited species to interact and hence for CO_2 splitting to occur. It would therefore be assumed that packing material would cause a reduction in CO_2 conversion. However, as CO_2 undergoes adsorption onto the surface of the packing material, this effect may be at least partially compensated for [22, 32].

Both catalysts and packing material will interact with the plasma. Fully packing $BaTiO_3$ and glass beads into the discharge gap have been shown to beneficially modify the discharge mode for the CO_2 decomposition reaction when used as a packing material, resulting in an increase in the average electric field and mean electron energy due to the formation of surface discharges alongside the typical filamentary discharges formed in the absence of a packed bed [22]. The extent of filamentary discharge formation is reduced in a packed-bed reactor as this type of discharge can only be formed within the gaps between the pellets and between the pellets and reactor wall, rather than throughout the whole discharge area; instead, surface discharges form at pellet contact points and across the pellet surfaces [11, 22, 32]. The increase in electron energy and local electric field occurs at the bead contact points as the external electric field causes them to become polarized [19]. Breakdown occurs more readily as the electron temperature is higher than in an empty reactor due to greater acceleration of the electrons in the enhanced electric field [19, 22]. This leads to a more efficient usage of the applied electrical energy which contributes to maximizing the energy efficiency and conversion [19].

The presence of a catalyst can increase both energy efficiency and CO_2 conversion simultaneously [33]. This is partly due to the electron temperature increasing when a catalyst is employed, even though the input power remains constant [33]. As mentioned above, polarization of the dielectric material occurs, enhancing the local electric field which increases the electron temperature [19, 22, 33]. At the contact points, the electron temperature has been shown to increase fourfold in comparison to the electron temperature in an empty reactor [33]. Consequently, there is a more efficient transference of energy from the applied electric power to the electrons in the form of heat [33]. As CO_2 splitting occurs through excitation and dissociation and electron impact ionization when the electrons transfer energy to CO_2, these processes are also more efficient, leading to an increase in energy efficiency in the presence of a catalyst [33]. Recent works have shown that the combination of DBD plasma with a photocatalyst ($BaTiO_3$ and TiO_2) using a partial catalyst packing configuration significantly enhanced the conversion of CO_2 and energy efficiency by up to 250% at low temperatures (~150 °C) compared to the plasma conversion of CO_2 in the absence of a catalyst, as shown in Fig. 9.6 [29]. The presence of the catalyst pellets in the part of the discharge gap has been found to induce plasma physical effects, such as the enhanced local electric field by 10% due to the polarization of the catalytic materials which increases the electron temperature and produces more energetic electrons and reactive species. More importantly, this work has demonstrated that energetic electrons generated by the plasma have acted as the main driving force to activate both photocatalysts for CO_2 conversion, making a major contribution to the enhanced CO_2 conversion and energy efficiency, while the

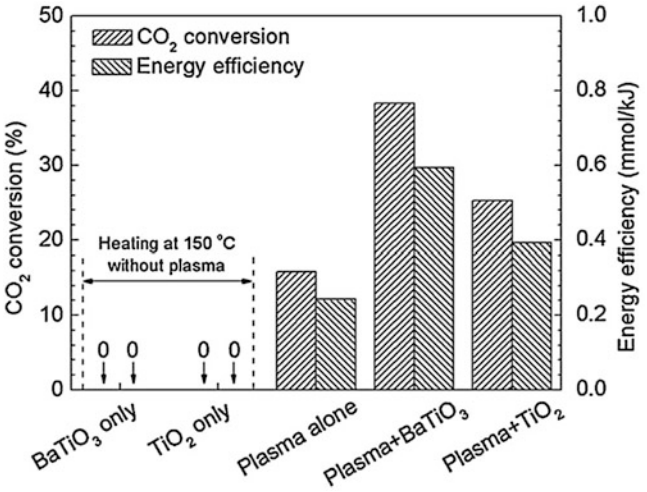

Fig. 9.6 Effect of photocatalysts ($BaTiO_3$ and TiO_2) on plasma conversion of CO_2 at a SEI of 28 kJ/L [29]

UV emission generated by the plasma has played a minor role in the activation of these photocatalysts for CO_2 conversion [29]. Thus, this exceptional synergistic effect resulting from the integration of DBD with photocatalysis for CO_2 conversion at low temperatures can be attributed to both the physical effect induced by the presence of the catalyst in the discharge and the dominant photocatalytic surface reaction driven by energetic electrons from the CO_2 discharge [29].

Furthermore, breakdown voltage is also affected by the packing material. In comparison to the breakdown voltage measured in a DBD reactor in the absence of a packing material (3.43 kV), the presence of glass beads has been shown to roughly halve this value (1.56 kV), while the use of $BaTiO_3$ has been shown to decrease breakdown voltage to less than a third (1.03 kV) [22]. Additionally, the decrease in electron density caused by the use of a dielectric material promotes oxygen radical recombination which in turn impedes the recombination of CO and O to form CO_2 [11, 34]. The reaction performance (CO_2 conversion and energy efficiency) is therefore enhanced due to the physical changes resulting from the presence of the packing material, with CO_2 conversion and energy efficiency increasing by up to 75% for a packed bed of $BaTiO_3$ (albeit not simultaneously) in comparison to no packing material [22]. However, not all packing material gives the same effect; quartz wool is very porous and interacts strongly with plasma, leading to the formation of intense filamentary discharges [22]. A summary of the energy efficiency achieved in different plasma-catalytic systems can be seen in Table 9.1. Also included are the energy efficiencies achieved without the use of a catalyst, in order to ascertain the effect of the catalyst. Clearly, different types of plasma system result in varying energy efficiencies (defined as (Eq. 9.3)) (Table 9.1). Generally, gliding arc and microwave plasmas attain higher energy efficiencies than DBDs;

Table 9.1 Comparison of CO_2 conversion and energy efficiency using different atmospheric pressure plasma sources

Plasma type	Packing materials/ catalysts	Maximum CO_2 conversion			Maximum energy efficiency			Ref
		SEI (kJ/L)	CO_2 conversion (%)	Energy efficiency (%)	SEI (kJ/L)	CO_2 conversion (%)	Energy efficiency (%)	
DBD	–	120	27.2	2.8	24	20.0	10.4	[18]
DBD	–	229.0	34.0	1.9	4.3	3.1	8.0	[12]
DBD	–	297.6	46.6	2.0	1.6	2.3	17.7	[35]
DBD	–	60.0	18.2	1.7	20.0	9.6	3.8	[36]
GAD	–	15.4	17.4	14.1	9.8	15.2	19.3	[37]
DBD	–	22.2	24.3	12.6	11.7	16.0	15.7	[38]
DBD	–	240.0	30.0	1.6	45.1	14.0	3.9	[10]
Corona	–	80	10.9	1.7	5.2	3.1	7.5	[39]
Microwave	NiO/TiO_2 (Ar plasma treated)	–	–	–	30	41.3	17.2	[40]
DBD	$BaTiO_3$	–	–	–	28	38.3	16.6	[29]
Packed-bed DBD	CaO	75.8	41.9	5.7	45.5	32.9	7.1	[41]
Packed-bed DBD	ZrO_2	240	42.3	4.6	36	9.6	9.6	[19]
Packed-bed DBD	$CaTiO_3$	52.9	20.5	4.8	32.4	15.8	6.1	[34]
Packed-bed DBD	$BaTiO_3$	60.0	28.2	5.9	24.0	13.7	7.1	[22]

however, DBDs are more easily combined with a catalyst and are more suited to industrial-scale applications.

The size and form of the packing material or catalyst can affect the reaction performance. If bead sizes are too small, the reaction performance can decrease in comparison to the reaction without packing. This is due to the decreased residence time, as well as the number of contact points being too great for the applied electrical energy to cause significant enhancement of the local electric field and the electron energy [19]. In one study that used a DBD reactor, CO_2 conversion generally increased with an increase in ZrO_2 bead size range (from 0.9–1 mm beads to 2–2.24 mm beads) at 80 W input power and various flow rates [19]. However, in another case, 0.18–0.25 mm beads of γ-Al_2O_3, MgO and CaO all resulted in a higher CO_2 conversion in comparison to larger beads with size range 0.25–0.42 mm [11]. The decrease in conversion for the larger beads was attributed to an increased void fraction causing a drop in the electric field strength and discharge area. As can be seen from just these two results with conflicting conclusions, the interactions between plasma and packing material are far from simple and many factors will contribute to reaction performance, making it difficult to predict the outcome for a particular system.

Another aspect which must be taken into account is the role the catalyst or packing material plays in the splitting of the CO_2 molecule via adsorption of the molecule onto the beads. Two types of adsorption can occur: chemical (occurs with materials such as CaO and MgO) and physical (such as for γ-Al_2O_3). Chemisorption leads to a higher CO_2 conversion as CO_2 molecules adsorbed this way more readily decompose [11]. Chemisorption is affected by the acid-base properties of the packing material, with high basicity materials leading to a greater CO_2 conversion as they aid adsorption. This is because highly basic metals are more easily reduced.

The number of surface oxygen vacancies present in the catalyst is a highly important factor for determining CO_2 conversion [29, 42], as dissociative electron attachment is facilitated by oxygen vacancies; hence a high number of vacancies can lead to an increase in CO_2 conversion (Fig. 9.7). Recently, Mei and his co-workers have shown that the presence of oxygen vacancies on the surface of $BaTiO_3$ and TiO_2 photocatalysts contributes to the enhanced CO_2 conversion in comparison to the plasma reaction without a catalyst [29]. They found that more oxygen vacancies were formed in $BaTiO_3$ than in TiO_2, resulting in the higher CO_2 conversion using $BaTiO_3$ in the plasma-catalytic conversion of CO_2 [29]. Various pretreatments of catalysts can also be used for the synthesis of a catalyst with a large number of oxygen vacancies. One study used plasma pretreatment, in which three different gases (CO_2, Ar and O_2) were used to treat NiO/TiO_2 catalysts [42]. Both O_2 and CO_2 pretreatments failed to result in a catalyst with high affinity for CO_2 decomposition; however, the Ar pretreatment led to a catalyst that increased both the energy efficiency and CO_2 conversion by a factor of 2 in comparison to the plasma-alone process. This difference in reaction performance between the catalysts prepared using different gases was attributed to the increase in the number of oxygen vacancies in the Ar-treated catalyst. This is because dissociative electron attachment occurs at the oxygen vacancy sites as CO_2 is adsorbed more easily here than on

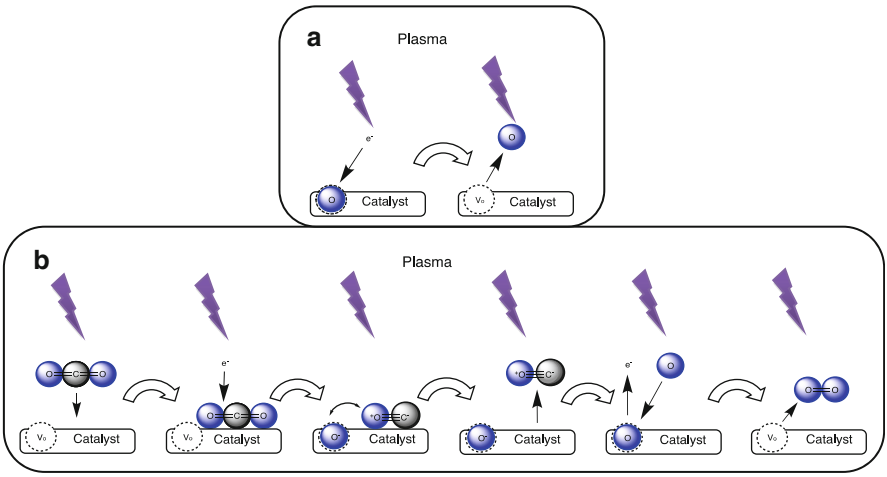

Fig. 9.7 (**a**) Generation of oxygen vacancies (V_o) at the catalyst surface via bombardment with plasma-generated electrons; (**b**) CO_2 dissociation mechanism via dissociative electron attachment at the catalyst surface

defect-free sites [42]. CO_2 can then be dissociated to CO and O^-, through the transient CO_2^- ion, due to electrons from the plasma colliding with the molecule. The CO molecule is then desorbed from the active site and the O^- ion releases an electron as it fills the oxygen vacancy on the catalyst surface [42]. Furthermore, the oxygen vacancies are regenerated, preventing any decrease in catalytic activity [42]. This could be due to a gaseous oxygen atom in the plasma recombining with surface-adsorbed O_2, according to (9.R6). As oxygen atoms in the plasma can also be in excited states, the recombination process may occur to an even greater extent due to this enhanced energy state [42]:

$$O_{ads} + O(g) \rightarrow O_2(g) \tag{9.R6}$$

9.3 Plasma Dry Reforming of CH_4 with CO_2

$$CO_2 + CH_4 \rightarrow 2CO + 2H_2 \tag{9.R7}$$

Dry reforming of methane with CO_2 (9.R7) has the benefit of utilizing two greenhouse gases in the form of different sources (e.g. landfill gas, biogas and shale gas) in a single process. This process usually produces syngas, a mixture of hydrogen and carbon monoxide, alongside other valuable chemicals and fuels. Syngas is a vital chemical intermediate that can be used to produce a variety of chemicals and fuels, including via the Fischer-Tropsch process. Higher hydrocarbons, such as C_2H_2, C_2H_4, C_2H_6 and C_3H_8, can also form from the dry reforming

reaction, although the concentration of these is always much smaller than that of syngas [43–45].

Very recently, Wang et al. have developed a water electrode DBD plasma reactor for the direct, one-step reforming of CH_4 with CO_2 into higher-value liquid fuels and chemicals (e.g. acetic acid, methanol, ethanol and formaldehyde) with high selectivity at room temperature (30 °C) and atmospheric pressure (Fig. 9.8) [46]. The total selectivity to oxygenates was approximately 50–60%, with acetic acid being the major liquid product at 40.2% selectivity. Two possible reaction pathways could contribute to the formation of acetic acid in this process. CO can react with a CH_3 radical to form an acetyl radical (CH_3CO) with a low energy barrier of 28.77 kJ/mol, followed by recombination with OH to produce acetic acid with no energy barrier. Direct coupling of CH_3 and carboxyl radicals (COOH) could also form acetic acid based on density functional theory (DFT) modeling. A few groups have also found the formation of trace oxygenates (e.g. alcohols and acids) as by-products of syngas production in plasma dry reforming of methane. In a DBD reactor, acetic, formic, butanoic and propanoic acids have all successfully been formed, along with methanol and ethanol [43]. There are a number of pathways through which formic acid and propanoic acid could form. The most likely pathway is the addition of CO to an ethyl radical, although an ethyl radical may also couple with a carboxyl radical; furthermore, the carboxyl radical could couple with a hydrogen radical to form formic acid. The carboxyl radicals required for acid formation are thought to result from the addition of CO and OH [43].

Carbon nanomaterials are also possible by-products of the dry reforming reaction (Fig. 9.9). Multiwall carbon nanotubes and spherical carbon nanoparticles have been formed in a gliding arc reactor [4]. These are important by-products as carbon

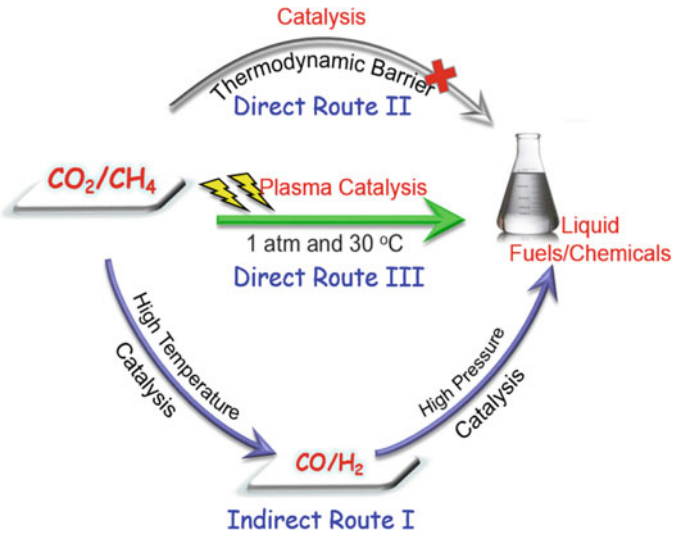

Fig. 9.8 Direct and indirect dry reforming of methane to liquid fuels and chemicals [46]

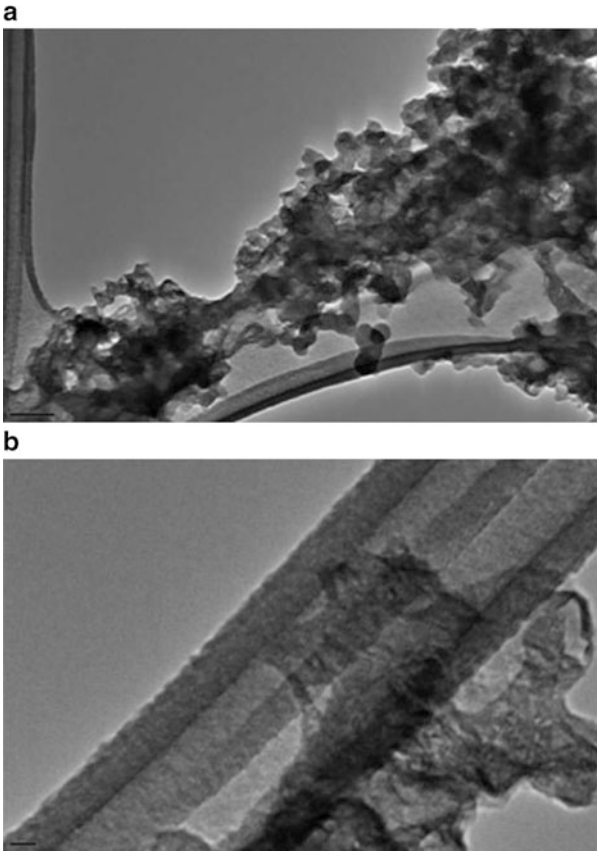

Fig. 9.9 TEM images of carbon nanomaterials formed in the plasma dry reforming of CH_4 and CO_2 using a gliding arc plasma: (**a**) spherical carbon nanoparticles and (**b**) carbon nanotubes [4]

nanotubes have a variety of applications; this could prove a sustainable and energy-efficient method for their production if further research is focused in this area [4].

9.3.1 Influence of Process Parameters

The influence of a wide range of operating parameters on the energy efficiency and conversions of reactants has been investigated using different plasma systems. The reactant conversion and the H_2/CO molar ratio, along with the product yields and selectivities, are affected by the molar ratio of CO_2/CH_4 in the feed [47, 48]. An increase in CO_2 content in the feed leads to a rise in both energy efficiency and total conversion [5, 49, 50]. This is because CO_2 and CH_4 decomposition occur via electron impact dissociation, forming O and H atoms, respectively. These atoms in turn react with each other to form OH, thus limiting the recombination of CH_3 and H and increasing CH_4 conversion [5].

One important factor that determines reaction performance is the number of micro-discharge filaments that come into contact with the gas molecules in the DBD, with a greater number of lower-energy filaments resulting in an increase in energy efficiency and conversion [5]. It has been reported that duty cycle affects CO_2 and CH_4 conversion in a DBD, with conversion increasing with duty cycle, when a sinusoidal voltage with square wave modulation is applied [43]. Pulsed plasma has been shown to effectively enhance the performance of the dry reforming process, with an increase in pulse frequency or applied peak voltage leading to higher total conversion [48, 51].

An increase in plasma power results in higher total conversion as a greater number of higher-energy electrons are formed, which can go on to initiate reactions [5]. However, input power can also affect product distribution, with a greater concentration of carbon powder and water forming at higher power. The use of a longer residence time can also increase total conversion, as the SEI is increased; however, it bears almost no impact on CO and H_2 selectivities [5, 48]. The SEI term incorporates both power and residence time, and if both parameters are adjusted but the SEI remains constant, the change in total conversion will be negligible [5]. However, an increase in SEI leads to higher CO_2 and CH_4 conversions in a variety of plasmas (gliding arc, DBD, corona), but has the opposite effect on the energy efficiency, resulting in a trade-off between the two [5].

Optical emission spectroscopic diagnostics has been used to understand the formation of a wide range of reactive species generated in the reforming process [27], while plasma chemical kinetic modeling has been used to understand the underlying plasma chemistry and reaction pathways of the dry reforming process [45]. The latter model demonstrates how selectivity towards different products can be achieved through manipulation of the residence time due to the spatially averaged densities of some molecules continually increasing with residence time, while others peak at a certain value [45].

In order to maximize reactant conversion and energy efficiency, the process parameters must be optimized. This is a difficult task as each plasma system will have a different set of optimal parameters and numerous experiments must be carried out to realize these. Alternatively, a modeling approach can be used. Some models have now shown good agreement with experimental results, even though they are much simplified versions of the actual plasma chemistry. As mentioned previously, a trade-off exists between energy efficiency and reactant conversion; hence a middle ground must be found that results in a viable process.

9.3.2 Catalytic Reforming Versus Plasma-Catalytic Reforming

As shown by 9.R7, dry reforming is a highly endothermic process. As such, high temperatures are required (>1000 °C) in the thermal process to overcome the stability of both the CO_2 and CH_4 molecules. A catalyst can be used to convert the

reactants at lower temperatures; however, reactions temperatures must still be above 700 °C [47, 52]. Carbon deposition can also occur on the catalyst surface, leading to catalyst deactivation [47, 52]. Both these issues incur cost, as the energy input must be high and catalysts must be replaced periodically. In order to overcome these issues, catalysts can be combined with NTP. In the plasma-catalytic system, the benefits of using NTP which can overcome the high stability of the CO_2 and CH_4 molecules at low temperature and atmospheric pressure, along with those of catalysis (reduction in activation barrier, increased selectivity and conversion), can be realized simultaneously. This can increase reaction performance [53, 54], as well as reducing costs. Furthermore, interactions occur between the catalyst and the plasma which can lead to a synergistic effect in terms of conversion and energy efficiency [47, 55]. However, coking can still be an issue in plasma-catalytic systems, although this may be dampened through removal by excited hydrogen species [53]. One method to overcome this is to flow pure CO_2 through the reactor to remove the deposited carbon [53]. The oxidation of carbon by CO_2 occurs much faster in a DBD reactor than a thermal one [53].

Thermal-catalytic and plasma-catalytic dry reforming differ in the reagent conversion ratio. Conversions of both CO_2 and CH_4 should be equal due to the stoichiometry of the reaction; however, as a result of the reverse water-gas shift reaction, in the thermal process, a higher conversion of CO_2 occurs in comparison to CH_4. This differs to the plasma reaction, in which the CH_4 conversion is higher. This can be attributed to the prevalence of gas-phase reactions that lead to the dissociation of the CH_4 molecule (9.R8, 9.R9, and 9.R10), as well as the production of CO_2 via 9.R11 [47]:

$$CH_4 + e \rightarrow CH_3 + H + e \tag{9.R8}$$

$$CH_4 + e \rightarrow CH_2 + H_2 + e \tag{9.R9}$$

$$CH_4 + e \rightarrow CH + H + H_2 + e \tag{9.R10}$$

$$CO_2{}^+ + CH_4 \rightarrow CH_4{}^+ + CO_2 \tag{9.R11}$$

As mentioned above, in the plasma-catalytic dry reforming reaction, plasma reactions occur in the gas phase to dissociate CH_4 (9.R8, 9.R9, 9.R10, and 9.R11) and CO_2 (9.R12) [51]:

$$CO_2 + e \rightarrow CO + O + e \tag{9.R12}$$

Active species created in the plasma can also adsorb onto the catalyst surface, from where they can form CO and H_2 products [55]:

$$CH_x + \square \rightarrow (CH_x)_{ad} \tag{9.R13}$$

$$H + \square \rightarrow H_{ad} \tag{9.R14}$$

$$O + \square \rightarrow O_{ad} \tag{9.R15}$$

$$(CH_x)_{ad} + O_{ad} \rightarrow CO_{ad} + xH_{ad} \quad (9.R16)$$

$$CO_{ad} \rightarrow CO + \square \quad (9.R17)$$

$$2H_{ad} \rightarrow H_2 + \square \quad (9.R18)$$

where □ is an empty adsorption site present on the catalyst surface. The simultaneous occurrence of both plasma and surface reactions in plasma-catalytic systems at low temperature can lead to synergy in terms of product selectivities and reactant conversions, which cannot occur in the catalytic process at low temperature due to insufficient energy input. Desorption of the species on the surface of the catalyst can also occur more readily in the plasma process as the plasma can affect the catalyst properties [55]. Thus, the plasma-catalytic process is more beneficial due to increased CO_2 and CH_4 conversion and product selectivities and a reduction in coking at lower energy input than the thermal catalytic process.

9.3.3 *Influence of Catalyst*

In the thermal catalytic dry reforming process, supported metal catalysts have been used widely, with non-noble metals being prevalent due to their low cost and wide availability. Catalysts with high activity for the thermal catalytic process have been used as the starting point for the plasma-catalytic process. Supported metal catalysts with a core and shell structure have been investigated as this allows the active sites to be uniformly distributed, while deactivation due to carbon deposition and sintering is kept to a minimum as a result of the strong interactions between the core and shell [56]. Zeolite 3A [57], NaX and NaY [58, 59], Ni/γ-Al_2O_3 [27, 30, 47, 60–62], Co/γ-Al_2O_3 [47], Mn/γ-Al_2O_3 [47], Ag/Al_2O_3 [63], Pd/Al_2O_3 [63, 64], Cu/Al_2O_3 [47, 64], Fe/Al_2O_3 [65], La_2O_3/γ-Al_2O_3 [66], $LaNiO_3$ [67], Cu-Ni/Al_2O_3 [55] and $LaNiO_3$@SiO_2 [56, 68] catalysts have all been tested in the plasma-catalytic process, with Ni/γ-Al_2O_3 being the most commonly used. More recently, K-, Mg- and Ce-promoted Ni/γ-Al_2O_3 catalysts have also been evaluated in plasma-catalytic dry reforming of methane and CO_2 [69]. However, the scope of catalysts available that are active for the thermal process has only just been touched upon for plasma dry reforming.

In the plasma-catalytic system, the catalyst structure can be influenced by the plasma, while the presence of the catalyst can affect the discharge properties [70, 71]. As a result of the interactions between the plasma and the catalyst, a synergistic effect can result, whereby the reaction performance is greater than the sum of the plasma-alone and the purely catalytic processes [27, 55]. The formation of radicals in the plasma can change the catalysts reaction mechanism as these species are adsorbed onto the catalyst surface, while adsorbed vibrational excited species can facilitate CO_2 and CH_4 dissociation through dissociative adsorption due to their high internal energies [55, 70]. It may also be possible that the catalytic activity is improved due to the charged particles on the catalyst surface and the

applied voltage acting similarly to the electrochemical promotion of catalysis [70]. Other plasma influences include changing the lattice structure of the catalyst due to the transference of thermal energy from ions and electrons causing thermal perturbation which can increase coking resistance and catalyst activity, as well as structural changes due to particle bombardments which lead to changes in catalyst pores, active metals and promoters [70]. One such change that can occur is in the crystallinity of the active metal and support due to variation in valence state, resulting in an increase in oxygen affinity which leads to greater conversion of CH_4 [70].

The changes discussed this far are a result of the plasma changing the properties of the catalyst. As mentioned above, the catalyst can also affect the plasma properties [53, 70]. Catalysts change the discharge mode to a combination of micro-discharge and surface discharge [71]. An increase in the local electron density due to energy concentrating in the gaps between the catalyst pellets results in an increase in reactions occurring in both the plasma and at the catalyst surface as the electric field is enhanced [70]. The dielectric constant of the catalyst also affects the plasma, with a high dielectric constant catalyst resulting in an increase in the plasma electric field [53, 70, 71]. High dielectric catalysts, such as ferroelectrics, can increase the production of syngas in the dry reforming reaction [70]. The catalyst properties, such as dielectric constant, and geometry are therefore highly important in determining reaction performance [54, 72]; thus, the reaction performance can be optimized through selection of catalyst.

Packing geometry can also influence the interactions between the plasma and the catalyst; in a DBD reactor, partially packing a Ni/γ-Al_2O_3 catalyst into the discharge gap results in an enhancement in reaction performance in comparison to a fully packed reactor [27, 30]. This is because the discharge in the partially packed reactor retains the strong filamentary discharge, whereas the reduction in discharge volume in the fully packed reactor changes the discharge mode to surface discharge and spatially limited micro-discharge [27].

In a DBD reactor, the use of a Ni/γ-Al_2O_3 catalyst has been shown to enhance the conversion of CH_4, along with the yield of CO and H_2, in comparison to the plasma-alone process; however, the CO_2 conversion decreased slightly upon addition of the catalyst [47]. This Ni/γ-Al_2O_3 catalyst resulted in higher H_2 and CO yields and CH_4 conversion than the Co/γ-Al_2O_3, Cu/γ-Al_2O_3 and Mn/γ-Al_2O_3 catalysts that were also tested in this reactor, with a maximum CH_4 conversion of 19.6% being achieved at a flow rate of 50 ml/min and 7.5 W discharge power [47]. Although the energy efficiency of the plasma reaction is not always increased by the addition of a catalyst, such as is the case when Co/γ-Al_2O_3 or Cu/γ-Al_2O_3 catalysts are used, both Ni/γ-Al_2O_3 and Mn/γ-Al_2O_3 catalysts were found to enhance the energy efficiency [47].

Energy efficiency is higher in gliding arc discharge in comparison to other types of discharge, and catalysts can increase this still further [54]. The use of a NiO/Al_2O_3 catalyst, placed in the afterglow of the discharge in a gliding arc reactor, was found to increase energy efficiency by over 20% in comparison to that achieved using plasma only [54]. H_2 yield, along with CO_2 and CH_4 conversions, was also increased. The concentration of active metal was found to influence reaction

performance, as a 33wt% NiO/Al_2O_3 catalyst resulted in a decrease in reaction performance in comparison to an 18wt% NiO/Al_2O_3 catalyst, while a smaller catalyst diameter was found to be beneficial [54].

The addition of dopants and use of bimetallic catalysts have also been studied. Zhang et al. investigated the effect of varying the concentrations of Cu and Ni in various Cu-Ni/γ-Al_2O_3 catalysts and found that the 12 wt% Cu-12 wt % Ni/γ-Al_2O_3 catalyst gave the optimum results for both CH_4 and CO_2 conversion (Fig. 9.10) [55]. This catalyst also achieved the maximum selectivity to CO of 75%. However, this selectivity was also achieved when using the 5 wt% Ni-12 wt% Cu/γ-Al_2O_3 catalyst, whereas the maximum selectivity to H_2 was achieved with 16 wt% Ni-12 wt % Cu/γ-Al_2O_3 and 20 wt% Ni-12 wt% Cu/γ-Al_2O_3 catalysts [55].

Another factor which must be taken into consideration is the catalyst support, as the support, along with the interactions between it and the active metal, can affect the reaction performance. A study completed by Mei et al. investigated the use of a Ni catalyst supported on γ-Al_2O_3, TiO_2, MgO and SiO_2 [73]. The results of this experiment concluded that the γ-Al_2O_3 support was most beneficial on the reaction performance, giving the highest CO_2 (26.2%) and CH_4 (44.1%) conversions, as well as the maximum achieved energy efficiency and highest yields of CO and H_2. This was attributed to the increased reducibility of the Ni/γ-Al_2O_3 catalyst and the number of stronger basic sites present at its surface (which facilitate CO_2 chemisorption and activation), along with its higher specific surface area and greater dispersion of smaller NiO particles [73]. Carbon deposition also occurred to a lower extent on this catalyst, as the increase in CO_2 chemisorption and activation may have resulted in adsorbed CO_2 undergoing gasification by surface-adsorbed oxygen [73]. Weaker interactions between the catalyst and support are favorable as this increases the reducibility of the catalyst, increasing its activity [27].

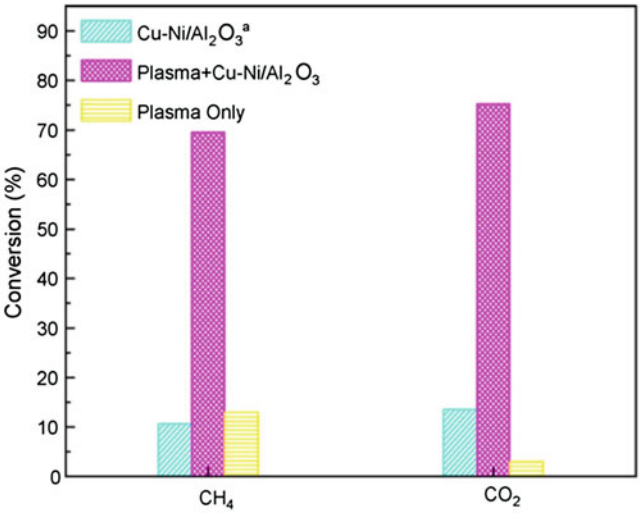

Fig. 9.10 Conversion of CH_4 and CO_2 in the dry reforming reaction using three different processes (plasma only, catalysis only and plasma catalysis) [55]

9.4 Plasma CO_2 Hydrogenation

A particularly significant route being developed for CO_2 conversion is CO_2 hydrogenation, which has a lower thermodynamic limitation compared to direct CO_2 decomposition and dry reforming of methane. Carbon dioxide can be hydrogenated in plasma via reaction with hydrogen at atmospheric pressure, thus avoiding the use of high pressure required by conventional thermal catalytic processes. CO_2 methanation (9.R20) and the reverse water-gas shift (RWGS) reaction (9.R19) prevail when hydrogen is reacted with CO_2 in the plasma process [74]; however, it is also possible to produce higher-value chemicals and fuels such as methanol and ethanol [75]. The main barrier to this process is the source of hydrogen. In order for this process to be both economically viable and sustainable, hydrogen must be produced using a low-cost, environmentally friendly and sustainable process. Currently, coal gasification and steam reforming of methane dominate the production pathways of H_2, leading to the emission of CO_2 [76]. Due to this, CO_2 conversion using hydrogen must convert a greater amount of CO_2 than hydrogen production pathways generate [76]. In thermal catalysis, the production of methane from H_2 and CO_2 is not considered a viable method of fuel production due to the low energy per unit volume and high H_2 consumption [77]. As plasma processes have the potential to convert large amounts of CO_2 at high energy efficiencies, interest is increasing into the development of these systems. In comparison to thermal CO_2 hydrogenation which requires high temperature and high pressure (30–300 bar), plasma systems operate at room temperature and pressure, hence increasing their viability. If plasma systems can be combined with a sustainable source of hydrogen, such as from water splitting using renewable energy, or indeed be used to split the hydrogen source in situ, this could prove a vital pathway for CO_2 mitigation.

9.4.1 CO_2 Hydrogenation to CO

$$CO_2 + H_2 \rightarrow CO + H_2O \tag{9.R19}$$

The conversion of CO_2 in this reaction has been found to rise as the H_2 content in the feed is increased. A higher ratio (H_2/CO_2) can also increase CO selectivity and yield, with a ratio of 4:1 resulting in a slight increase in CO selectivity and a threefold increase in CO yield in comparison to a feed ratio of 1:1 in a DBD [74]. Furthermore, this increase in feed ratio also results in a rise in CO production efficiency.

The selectivity to CO has been found to increase with a rise in total flow rate [78]. This is most likely due to the decreased residence time associated with an increase in flow rate resulting in the recombination of CO and O being suppressed, along with the further hydrogenation of CO to form hydrocarbons. This hypothesis is

supported by the decrease in selectivity to CH_4 that occurs as the total flow rate is raised, as detailed below.

In order to enhance the production of CO, a catalyst can be added into the reactor. In a DBD reactor, it was found that the addition of a Mn/γ-Al_2O_3 catalyst leads to an increase (of 114%) in CO yield in comparison to the plasma-alone process, as well as an increase (of 116%) in CO production efficiency [74].

9.4.2 CO_2 Hydrogenation to CH_4

$$CO_2 + 4H_2 \rightarrow CH_4 + 2H_2O \tag{9.R20}$$

In this process, a higher H_2 content in the feed in comparison to CO_2 is desirable as this increases the conversion of CO_2. This has been determined both experimentally [74, 79] and through the use of a 1D fluid model [76]. A 3:1 ratio (H_2/CO_2) is optimal for enhancing CH_4 yield [74]. Optimizing the total flow rate can also maximize the CH_4 selectivity and CO_2 conversion. A very low total flow rate can lead to reverse reactions occurring, reforming CO from CH_4 according to 9.R21, due to the longer residence time increasing the interactions between the CO_2 hydrogenation products and the excited species in the plasma [78]:

$$CH_4 + H_2O \rightarrow CO + 3H_2 \tag{9.R21}$$

As the total flow rate is increased, the rate of formation of CH_4 becomes larger than the rate of the reverse reaction, leading to an increase in CH_4. At high total flow rates however, the residence time is too low for reagent gases to interact with excited plasma species, decreasing the overall production of CH_4 as both the forward and reverse reactions occur to a lesser extent [78].

For DBD plasmas, the use of an alumina reactor instead of quartz is beneficial on reaction performance due to the enhanced relative dielectric permittivity coefficient of alumina [79].

Addition of a magnetic field can enhance CO_2 conversion, increasing the CH_4 selectivity by over 10% at a discharge power of 30 W while also tripling the energy efficiency of the process [80]. This study however employed low pressure (200 Pa), reducing simplicity of design and requiring extra energy input, thus detracting from the benefits of NTP. The function of the magnetic field is to prevent electrons from diffusing to the downstream region. In the downstream region, CH_4 is produced but also decomposed through electron impact dissociation (Eq. 9.4), leading to a decrease in the yield of CH_4 [80]. Magnetized electrons cannot travel out of the magnetic field; hence the downstream recombination reaction is suppressed, while CH_4 production can still proceed via reactions involving neutral radicals as these are not magnetized. The magnetic field also increases the electron density, due to

confinement of the electrons in the magnetic field, which leads to an increase in the CO_2 decomposition reaction as well as the energy efficiency [80].

An increase in power input generally results in a higher selectivity to CH_4 due to the increase in power density this results in [79, 80]. However, it has been found that at high-power input (>160 W), energy is transferred to the electrodes through heating rather than being used for plasma production, resulting in no further increase in CH_4 selectivity [80]. A rise in voltage also causes an increase in plasma density, which again leads to an increase in CH_4 selectivity. In radio frequency (RF) discharge, the relationship between CH_4 concentration and voltage can be expressed as [78]:

$$[CH_4] \propto (V)^N \ (N \geq 2) \tag{9.4}$$

Hence at higher voltages, the production efficiency of CH_4 increases. A study into the CH_4 production dependence on the repetition frequency of a low-pressure RF discharge has shown that CH_4 yield increases with repetition frequency [78]. The production of CO increases linearly with repetition frequency (up to its saturation point) due to an increase in the number of electrons as CO is formed via electron impact dissociation of CO_2 [78]. CH_4 is formed via reaction between CO and H; hence there is a power law relationship between the formation of CH_4 and the repetition frequency (and number of electrons) [78].

A smaller discharge gap is beneficial on the CO_2 conversion and CH_4 selectivity due to the rise in input power density caused by enhancement in the electric field [80]. In fact, a smaller discharge gap can achieve the same CH_4 selectivity at a lower input power than when using a larger discharge gap [80]. A reduction in discharge gap can also increase the production efficiency of the system. It must be noted here that for the case of [80], a decrease in discharge gap also resulted in an increase in magnetic field.

As expected, an increase in power input results in a decreased energy efficiency [80]. However high-power inputs give rise to larger conversions. Catalysts have therefore been employed as a method to combat this trade-off. The use of Mn/γ-Al_2O_3 and Cu/γ-Al_2O_3 catalysts in a coaxial DBD reactor has been found to increase CO_2 conversion as well as the energy efficiency of both CH_4 and CO production in comparison to the plasma-alone process [74]. The Cu/γ-Al_2O3 catalyst was found most beneficial for the production of CH_4 as this catalyst achieved the highest yield and selectivity to CH_4, while the maximum CO_2 conversion was achieved using the Mn/γ-Al_2O_3 catalyst. However, the Mn/γ-Al_2O_3 catalyst resulted in a decrease in CH_4 selectivity in comparison to the process in the absence of a catalyst. The decrease in CO_2 conversion attained when using the Cu/γ-Al_2O_3 catalyst in comparison to the Mn/γ-Al_2O_3 catalyst may be attributed to the increased prevalence of the water gas shift reaction in the presence of this catalyst as Cu catalysts are often used for catalyzing this reaction; hence the apparent CO_2 conversion will be reduced [74]. It is therefore important to select a catalyst that will suppress the water gas shift reaction and simultaneously increase the CO_2 conversion and the selectivity to CH_4.

The combination of plasma and catalysis allows the CO_2 methanation reaction to occur at much lower temperatures than those required in the purely catalytic process [81]. Below 250 °C, negligible CO_2 conversion occurs for the catalytic process; however, when combined with plasma, the CO_2 conversion reaches 80%, with 90% selectivity to CH_4, for the addition of a Ce-Zr supported Ni catalyst in a DBD reactor [81]. This is due to the creation of excited species in the plasma, which generate new pathways for CO_2 dissociation; hence the reaction is not limited by the rate of CO_2 dissociation at the catalyst surface as it is in the purely catalytic process [82]. The use of nickel-containing hydrotalcite catalysts has also shown promise in the plasma-catalytic CO_2 methanation reaction, with a CO_2 conversion of 80% and selectivity to CH_4 of nearly 100% having been achieved in a DBD reactor [83]. It is thought that the high number of low- and medium-strength basic sites is responsible for the high activity of this catalyst, as when promoted with metals containing high-strength basic sites (Ce and Zr), the conversion and yield decrease and no other important morphological changes could be identified [83].

9.4.3 Pathways of CO and CH_4 Formation

In order for methane to form, CO_2 is first dissociated to CO. Reaction between CO and H_2 can then occur to form CH_4. However, the oxygen radical produced in the dissociation of CO_2 will compete to react with hydrogen, forming water [84].

The dominating pathway for production of CO occurs via electron impact dissociation of CO_2 (9.R12). At low CO_2 concentrations in the feed, electron impact dissociation is also the main pathway for the dissociation of H_2 (9.R22); however, at high CO_2 concentrations, H_2 is mostly consumed through reaction with H_2O^+ and H_3O^+ [76]:

$$H_2 + e \rightarrow H_2^* \rightarrow H + H \tag{9.R22}$$

Dissociation of CO can also occur; however, this reaction is highly endothermic; hence it occurs to a much lesser extent [78].

The net loss rate of CO_2 remains constant at all inlet concentrations, but the net loss rate of H_2 varies. At high H_2 concentrations, the net loss rate is high as there is more H_2 in the feed; as the H_2 concentration is decreased, the net loss rate follows the same trend [76]. The net loss rate of H_2 is higher than that of CO_2, with this effect being more pronounced at high H_2 concentrations.

Downstream of the reactor, electron energies have decreased and are usually insufficient for dissociation reactions. Recombination reactions prevail (9.R23 and 9.R24) as these exothermic reactions only require low-energy electrons [78]:

$$CO + 3H_2 \rightarrow CH_4 + H_2O \tag{9.R23}$$

$$CO + 2H_2 \rightarrow CH_3OH \quad (9.R24)$$

However, the dissociation of CH_4 can occur via electron impact dissociation (9.R25) [80], reducing the obtained yield:

$$CH_4 + e \rightarrow CH_x + (4 - x)H + e(x = 1, 2, 3) \quad (9.R25)$$

The water gas shift (WGS) reaction (9.R26) can also occur, decreasing the apparent CO_2 and H_2 conversions [74]:

$$CO + H_2O \rightarrow CO_2 + H_2 \quad (9.R26)$$

In this simplified summary of reaction pathways, it can therefore be seen that the formation of CH_4 occurs via CO formation, which forms as a result of CO_2 dissociation. Methanol is also a possible product. Unwanted reactions also occur in the plasma system, such as the water gas shift reaction and the dissociation of CH_4; hence these reactions must be suppressed to ensure high yields of CO and CH_4.

9.4.4 *CO_2 Hydrogenation to Liquid Fuels*

CO_2 hydrogenation to liquid fuels (e.g. methanol, ethanol and dimethyl ether (DME)) is one of the most attractive routes for CO_2 conversion and utilization (Fig. 9.11). Significant efforts have been concentrated on CO_2 hydrogenation to methanol (9.R27) using heterogeneous catalysis at high pressures [85]. CH_3OH is a valuable fuel substitute and additive and is also a key feedstock for the synthesis of other higher-value chemicals. In addition, methanol is considered a promising hydrogen carrier, suitable for storage and transportation [85]:

$$CO_2 + 3H_2 \rightarrow CH_3OH + H_2O \quad (9.R27)$$

Cu-based catalysts have attracted considerable interest for catalytic hydrogenation of CO_2 to methanol, owing to the excellent activity of metallic Cu for this reaction. Extensive efforts have also been devoted to modifying the structure of Cu-based catalysts using various supports (Al_2O_3, ZnO, ZrO_2, SiO_2, Nb_2O_5, Mo_2C and carbon materials, etc.), promoters (Zn, Zr, Ce, Ga, Si, V, K, Ti, B, F and Cr) and preparation methods [85–87].

Up until now, very limited research has concentrated on CO_2 hydrogenation using nonthermal plasmas, either with or without a catalyst [88–91]. The majority of this research reports CO as the dominant chemical, with CH_4 formed as a minor product and no CH_3OH detected [80–82]. In the late 1990s, Eliasson and co-workers investigated CO_2 hydrogenation to CH_3OH using a DBD plasma reactor [92]. However, only trace amounts of CH_3OH were produced, with a maximum CH_3OH yield

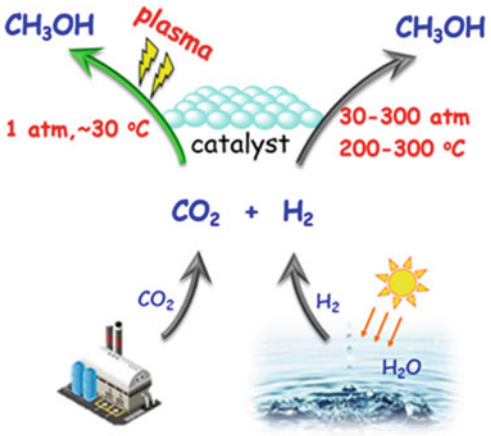

Fig. 9.11 Scheme of CO_2 hydrogenation to methanol [75]

of 0.2% obtained at atmospheric pressure (1 bar), a relatively high plasma power of 400 W, a total flow rate of 250 ml/min and a H_2/CO_2 molar ratio of 3:1. They also found that packing a $Cu/ZnO/Al_2O_3$ catalyst (a commercial methanol synthesis catalyst) in the discharge increased the methanol yield (from 0.1 to 1.0%), methanol selectivity (from 0.4 to 10.0%) and CO_2 conversion (from 12.4% to 14.0%) at a higher pressure (8 bar) under similar operating conditions [92]. However, the methanol yield and selectivity were still significantly lower than those reported in catalytic CO_2 hydrogenation processes. The formation of trace CH_3OH in plasma CO_2 reduction was also reported using a radio frequency impulse discharge at low pressures (1–10 torr) [78]. Very recently, Wang et al. developed a specially designed water electrode DBD reactor for the highly selective hydrogenation of CO_2 to methanol at room temperature (30 °C) and atmospheric pressure [75]. They found that the methanol production was strongly dependent on the structure of the DBD reactor; the DBD reactor with a special water electrode design and a single dielectric showed the highest reaction performance in terms of the conversion of CO_2 and methanol yield (Fig. 9.12) [75].

The combination of the plasma with $Cu/\gamma\text{-}Al_2O_3$ or $Pt/\gamma\text{-}Al_2O_3$ catalyst significantly enhanced the CO_2 conversion and methanol yield compared to the plasma hydrogenation of CO_2 without a catalyst. The maximum methanol yield of 11.3% and methanol selectivity of 53.7% were achieved over the $Cu/\gamma\text{-}Al_2O_3$ catalyst with a CO_2 conversion of 21.2% in the plasma-catalytic process, while no reaction occurred at ambient conditions without using plasma [75]. Compared to catalytic CO_2 hydrogenation to methanol, which has been carried out using a wide range of catalysts, very limited catalysts that are active for thermal catalytic process have been examined for plasma hydrogenation of CO_2. In addition, the production of dimethyl ether from plasma CO_2 hydrogenation was reported using an atmospheric pressure surface discharge with a CO_2 conversion of 15% and a H_2/CO_2 molar ratio of 1:1 [91].

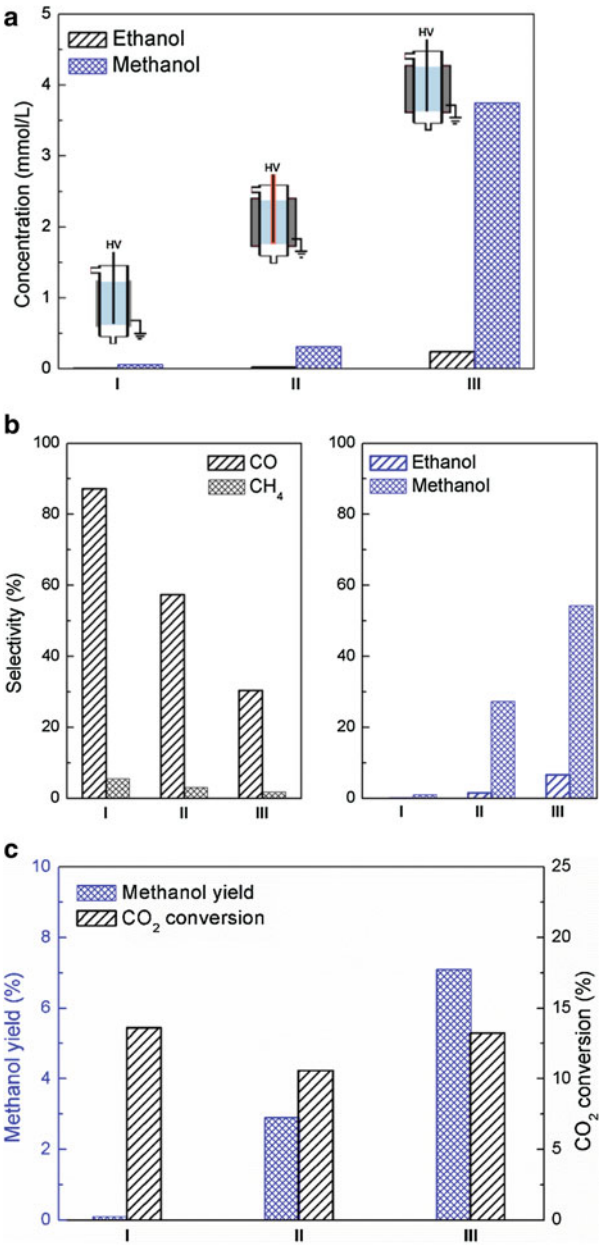

Fig. 9.12 Influence of reactor structure (reactor I, II and III) on plasma hydrogenation of CO_2 process: (**a**) concentration of oxygenates; (**b**) selectivity of gas and liquid products; (**c**) methanol yield and CO_2 conversion (reaction pressure 1 atm, H_2/CO_2 molar ratio 3:1) [75]

9.5 Plasma CO_2 Conversion with Water

Carbon dioxide can be hydrogenated with water to produce syngas [93, 94]. Limited research exists into this method of splitting CO_2. A higher H_2O content in the feed appears to be beneficial on the production of H_2, although the study citing this only uses ratios between 10:50 and 50:50 (H_2O/CO_2); hence it is unclear if further increasing the H_2O content will continue the trend [93]. The opposite is true for the production of CO [93].

SEI can affect product yields, with maximum H_2 yields occurring at low SEI [93]. A rise in the feed flow rate results in H_2 yields decreasing; this is expected due to the decrease in residence time and the relationship between SEI and flow rate discussed previously. The reduction in H_2 yield due to high SEI and/or increased flow rate can be attributed to the occurrence of the reverse water gas shift reaction, as the yield of CO remains constant [93]:

Syngas is not the only possible product of plasma CO_2 hydrogenation with water: methane can also be produced [94, 95]. Although the current obtainable methane concentration is low (ppm) and reported energy efficiencies are well below feasible, the proof of concept is important. Methane production from CO_2 and water using NTP could potentially provide a one-step process for creating a useful energy source from a sustainable source of hydrogen.

The addition of a catalyst to this reaction can remarkably increase the yield of methane, as dissociative adsorption of H_2, CO (formed via plasma gas phase reactions) and CO_2 occurs at the catalyst surface, enabling the hydrogenation of carbon species via this mechanism as opposed to through plasma gas-phase reactions alone [95]. The use of a NiO/Al_2O_3 catalyst is beneficial for the production of methane as this catalyst facilitates the hydrogenation of CO [94]. Furthermore, the use of a reduced Ni catalyst can facilitate the production of carbon nanofibers through plasma-assisted chemical vapor decomposition of methane (Fig. 9.13) [94].

The reduction of CO_2 using water is possible using electrochemical processes [96] as well as through photoreduction [97]. These processes produce methanol, an important chemical intermediate [96]. To the best of the authors' knowledge, this reaction has not been carried out using plasma processes; however, the production of methanol has been successful in a DBD (albeit in very small quantities) when using hydrogen in the feed [92]. The addition of a $CuO/ZnO/Al_2O_3$ catalyst has also been shown to increase the methanol yield by a factor of 10 [92]. As H_2O can be successfully split into H_2 in plasma, the production of methanol from CO_2 and H_2O is theoretically possible. The main competing reaction for the formation of methanol is the production of methane [92].

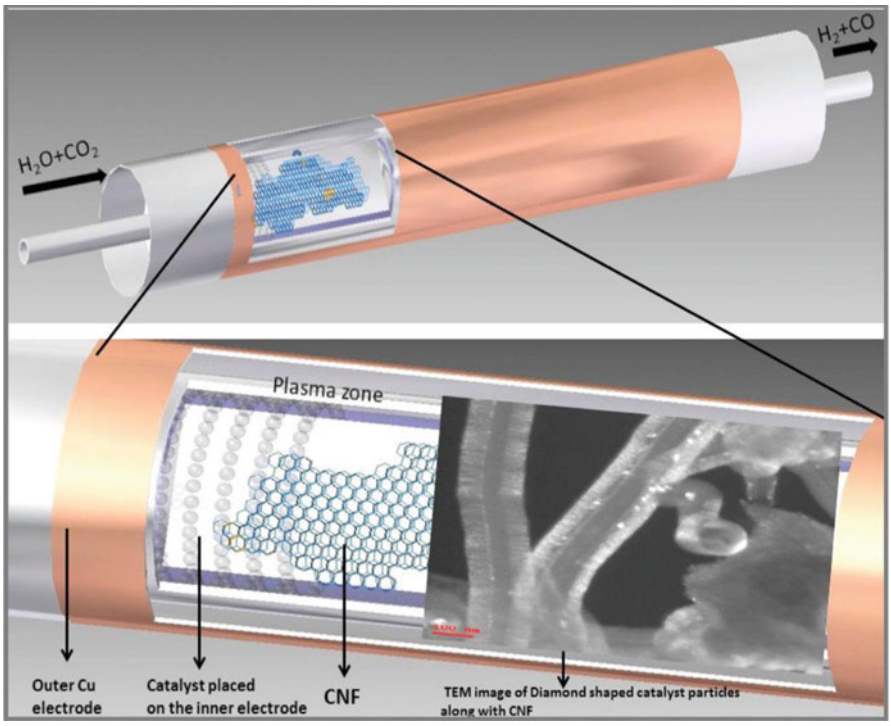

Fig. 9.13 Formation of CNF in the plasma conversion of CO_2 with water over Ni/Al_2O_3 catalyst [94]

9.6 Summary and Future Outlook

Plasma-based technologies for the conversion of CO_2 into value-added fuels and chemicals show great potential due to the ability of nonthermal plasma to break bonds in the highly stable CO_2 molecule while operating at room temperature and pressure. Plasma systems therefore have an advantage over thermal processes, which require high-temperature inputs; hence plasma conversion of CO_2 could prove much more feasible on an industrial scale. However, a trade-off between energy efficiency and CO_2 conversion currently exists in the plasma process as conversion increases when energy input is raised, which also causes a decrease in energy efficiency. Initial research has shown that this problem can be overcome by modifying the plasma system, such as by combining the plasma discharge with a catalyst; however, further research is required to promote the simultaneous increase of energy efficiency and conversion. Once plasma processes can concurrently operate at high conversion and energy efficiency, they will become a front runner in green technologies for the conversion of carbon dioxide.

Plasma chemistry is highly complex, and although much research is being conducted into plasma modeling, the models being used are greatly simplified

versions of the reactions taking place [16, 93, 98]. Newer models can also leave their predecessors redundant; therefore, further study is required to produce comprehensive models for a variety of plasma processes [99]. When it comes to plasma catalysis, the chemistry becomes even more complex due to the interactions occurring between the plasma and catalyst. The number of different catalysts that can be employed in plasma processes, along with variations in catalyst preparation method, loading amount, pretreatment, etc., makes it tricky to use a 'one-model-fits-all' approach. If a greater understanding of plasma reactions and the interactions between plasma and catalyst can be realized, a more comprehensive model could be produced. In situ experimental techniques, such as in situ infrared spectroscopy, can lead to a greater understanding of plasma-assisted surface reactions, for example, plasma adsorption or desorption on the surface of the catalyst. Using techniques such as this could help to create such a model, drastically reducing the time required to optimize a process and leading to selection of the optimum catalyst without the need for numerous laborious experiments.

The potential exists to produce more complex carbon-based liquid products using plasma. A variety of liquids can currently be produced in small quantities, such as formaldehyde, acetic acid and methanol, as well as ethylene and C_4 hydrocarbons [100, 101]. However, the selectivity to many of these products still needs to be improved for the process to be viable. The selection of an appropriate catalyst that can increase the selectivity to the required product is therefore required for progress to be made in this area.

Thermal catalytic techniques are currently used to produce liquid hydrocarbons such as DME from carbon dioxide and hydrogen. For the production of DME, high temperatures (240–270 °C) and pressures (3 MPa) are required [102–104]. If NTP at atmospheric pressure can be used instead, the energy input can be drastically reduced. In order to produce hydrocarbons directly from CO_2, bifunctional catalysts are required [105]. Novel catalysts and new reactor setups may help offset the need for high pressures in a plasma reactor. Much more research is needed to create plasma processes that produce liquid hydrocarbons currently only produced by other (non-plasma) techniques, but if successful these processes could transform the chemical and energy industries.

The scope and potential of plasma processes for the utilization of CO_2 are therefore vast. These processes reduce the concentration of CO_2 in our atmosphere and allow the chemical storage of energy which can be transferred to the system from renewable energy sources at peak times. As well as producing fuels, valuable chemicals can also be formed. A greater understanding of the plasma chemistry, both through modeling of plasma and coupling with other techniques such as catalysis, as well as further insight into synthesizing a catalyst which will create synergy when combined with plasma [106], will allow this field to expand. Alongside this, further research into the conversion of CO_2 in feed gases mixed with other gases from industrial waste streams could also be beneficial for creating large-scale plasma processes for industrial applications [24].

Acknowledgments The authors acknowledge financial support from the UK EPSRC SUPERGEN Hydrogen & Fuel Cell (H2FC) Hub (EP/J016454/1), EPSRC SUPERGEN Bioenergy Challenge II Programme (EP/M013162/1), and EPSRC Impact Acceleration Account (IAA). We acknowledge the funding from the European Union's Horizon 2020 Research and Innovation Programme under the Marie Sklodowska-Curie Action (Grant Number 823745).

References

1. IPCC. (2014). *Climate Change 2014: Mitigation of Climate Change*. Contribution of Working Group III to the Fifth assessment report of the intergovernmental panel on climate change, New York.
2. Snoeckx, R., & Bogaerts, A. (2017). Plasma technology: A novel solution for CO_2 conversion. *Chemical Society Review, 46*, 5805–5863.
3. Ashford, B., & Tu, X. (2017). Non-thermal plasma technology for the conversion of CO_2. *Current Opinion in Green and Sustainable Chemistry, 3*, 45–49.
4. Tu, X., & Whitehead, J. C. (2014). Plasma dry reforming of methane in an atmospheric pressure AC gliding arc discharge: Co-generation of syngas and carbon nanomaterials. *International Journal of Hydrogen Energy, 39*, 9658–9669.
5. Snoeckx, R., Zeng, Y. X., Tu, X., & Bogaerts, A. (2015). Plasma-based dry reforming: Improving the conversion and energy efficiency in a dielectric barrier discharge. *RSC Advances., 5*, 29799–29808.
6. Wang, J., Xia, G., Huang, A., Suib, S. L., Hayashi, Y., & Matsumoto, H. (1999). CO_2 decomposition using glow discharge plasmas. *Journal of Catalysis, 185*, 152–159.
7. Spencer, L. F., & Gallimore, A. D. (2011). Efficiency of CO_2 dissociation in a radio-frequency discharge. *Plasma Chemistry and Plasma Processing, 31*, 79–89.
8. Tsuji, M., Tanoue, T., Nakano, K., & Nishimura, Y. (2001). Decomposition of CO_2 into CO and O in a microwave-excited discharge flow of CO_2/He or CO_2/Ar mixtures. *Chemistry Letters, 1*, 22–23.
9. Aerts, R. (2014). *Experimental and computational study of dielectric barrier discharges for environmental applications*. Belgium: University of Antwerp.
10. Paulussen, S., Verheyde, B., Tu, X., De Bie, C., Martens, T., Petrovic, D., Bogaerts, A., & Sels, B. (2010). Conversion of carbon dioxide to value-added chemicals in atmospheric pressure dielectric barrier discharges. *Plasma Sources Science and Technology, 19*, 034015.
11. Duan, X., Hu, Z., Li, Y., & Wang, B. (2015). Effect of dielectric packing materials on the decomposition of carbon dioxide using DBD microplasma reactor. *American Institute of Chemical Engineers, 61*, 898–903.
12. Aerts, R., Somers, W., & Bogaerts, A. (2015). CO_2 splitting in a dielectric barrier discharge plasma: A combined experimental and computational study. *ChemSusChem, 8*, 702–716.
13. Wang, W. Z., Berthelot, A., Kolev, S., Tu, X., & Bogaerts, A. (2016). CO_2 conversion in a gliding arc plasma: 1D cylindrical discharge mode. *Plasma Sources Science and Technology, 25*, 065012.
14. Silva, T., Britun, N., Godfroid, T., & Snyders, R. (2014). Optical characterization of a microwave pulsed discharge used for dissociation of CO_2. *Plasma Sources Science and Technology, 23*, 025009.
15. Pietanza, L. D., Colonna, G., D'Ammando, G., Laricchiuta, A., & Capitelli, M. (2015). Vibrational excitation and dissociation mechanisms of CO_2 under non-equilibrium discharge and post-discharge conditions. *Plasma Sources Science and Technology, 24*, 042002.
16. Berthelot, A., & Bogaerts, A. (2016). Modeling of plasma-based CO_2 conversion: Lumping of the vibrational levels. *Plasma Sources Science and Technology, 25*, 045022.
17. Mori, S., & Tun, L. L. (2017). Synergistic CO_2 conversion by hybridization of dielectric barrier discharge and solid oxide electrolyser cell. *Plasma Processes and Polymers, 14*, 1600153.

18. Mei, D. H., He, Y. L., Liu, S. Y., Yan, J. D., & Tu, X. (2016). Optimisation of CO_2 conversion in a cylindrical dielectric barrier discharge reactor using design of experiments. *Plasma Processes and Polymers, 13*, 544–556.
19. Van Laer, K., & Bogaerts, A. (2015). Improving the conversion and energy efficiency of carbon dioxide splitting in a zirconia-packed dielectric barrier discharge reactor. *Energy Technology, 3*, 1038–1044.
20. Mei, D., & Tu, X. (2017). Conversion of CO_2 in a cylindrical dielectric barrier discharge reactor: Effects of plasma processing parameters and reactor design. *Journal of CO_2* Utilization, 19, 68–78.
21. Winanti, W. S., Purwanto, W. W., & Bismo, S. (2014). Decomposition of carbon dioxide in the three-pass flow dielectric barrier discharge plasma reactor. *International Journal of Technology, 1*, 1–11.
22. Mei, D., Zhu, X., He, Y. L., Yan, J. D., & Tu, X. (2015). Plasma-assisted conversion of CO_2 in a dielectric barrier discharge reactor: Understanding the effect of packing materials. *Plasma Sources Science and Technology, 24*, 015011.
23. Ramakers, M., Michielsen, I., Aerts, R., Meynen, V., & Bogaerts, A. (2015). Effect of argon or helium on the CO_2 conversion in a dielectric barrier discharge. *Plasma Processes and Polymers, 12*, 755–763.
24. Snoeckx, R., Heijkers, S., Wesenbeeck, K., Lenaerts, S., & Bogaerts, A. (2016). CO_2 conversion in a dielectric barrier discharge plasma: N_2 in the mix as helping hand or problematic impurity? *Energy & Environmental Science, 9*, 999–1011.
25. Heijkers, S., Snoeckx, R., Kozak, T., Silva, T., Godfroid, T., Britun, N., Snyders, R., & Bogaerts, A. (2015). CO_2 conversion in a microwave plasma reactor in the presence of N_2: Elucidating the roles of vibrational levels. *The Journal of Physical Chemistry C, 119*, 12815–12828.
26. Butterworth, T., Elder, R., & Allen, R. (2016). Effects of particle size on CO_2 reduction and discharge characteristics in a packed bed plasma reactor. *Chemical Engineering Journal, 293*, 55–67.
27. Tu, X., & Whitehead, J. C. (2012). Plasma-catalytic dry reforming of methane in an atmospheric dielectric barrier discharge: Understanding the synergistic effect at low temperature. *Applied Catalysis B: Environmental, 125*, 439–448.
28. Neyts, E. C., & Bogaerts, A. (2014). Understanding plasma catalysis through modelling and simulation—A review. *Journal of Physics D: Applied Physics, 47*, 224010.
29. Mei, D., Zhu, X., Wu, C., Ashford, B., Williams, P. T., & Tu, X. (2016). Plasma-photocatalytic conversion of CO_2 at low temperatures: Understanding the synergistic effect of plasma-catalysis. *Applied Catalysis B: Environmental, 182*, 525–532.
30. Tu, X., Gallon, H. J., Twigg, M. V., Gorry, P. A., & Whitehead, J. C. (2011). Dry reforming of methane over a Ni/Al_2O_3 catalyst in a coaxial dielectric barrier discharge reactor. *Journal of Physics D: Applied Physics, 44*, 274007.
31. Mei, D., & Tu, X. (2017). Atmospheric pressure non-thermal plasma activation of CO_2 in a packed-bed dielectric barrier discharge reactor. *ChemPhysChem, 18*, 3253–3259.
32. Ray, D., & Subrahmanyam, C. (2016). CO_2 decomposition in a packed bed DBD plasma reactor: Influence of packing materials. *RSC Advances, 6*, 39492.
33. Bogaerts, A., Kozak, T., van Laer, K., & Snoeckx, R. (2015). Plasma-based conversion of CO_2: Current status and future challenges. *Faraday Discussions, 183*, 217–232.
34. Yu, Q., Kong, M., Liu, T., Fei, J., & Zheng, X. (2012). Characteristics of the decomposition of CO_2 in a dielectric packed-bed plasma reactor. *Plasma Chemistry and Plasma Processing, 32*, 153–163.
35. Belov, I., Paulussen, S., & Bogaerts, A. (2016). Appearance of a conductive carb.onaceous coating in a CO_2 dielectric barrier discharge and its influence on the electrical properties and the conversion efficiency. *Plasma Sources Science and Technology, 25*, 015023.
36. Duan, X., Li, Y., Ge, W., & Wang, B. (2015). Degradation of CO_2 through dielectric barrier discharge microplasma. *Greenhouse Gases: Science and Technology, 5*, 131–140.

37. Indarto, A., Yang, D. R., Choi, J. W., Lee, H., & Song, H. K. (2007). Gliding arc plasma processing of CO_2 conversion. *Journal of Hazardous Materials, 146*, 309–315.
38. Ozkan, A., Dufour, T., Bogaerts, A., & Reniers, F. (2016). How do the barrier thickness and dielectric material influence the filamentary mode and CO_2 conversion in a flowing DBD? *Plasma Sources Science and Technology, 25*, 045016.
39. Xu, W., Li, M. W., Xu, G. H., & Tian, Y. L. (2004). Decomposition of CO_2 using DC corona discharge at atmospheric pressure. *Japanese Journal of Applied Physics, 43*, 8310–8311.
40. Chen, G. X., Georgieva, V., Godfroid, T., Snyders, R., & Delplancke-Ogletree, M.-P. (2016). Plasma assisted catalytic decomposition of CO_2. *Applied Catalysis B: Environmental, 190*, 115–124.
41. Duan, X. F., Hu, Z. Y., Li, Y. P., & Wang, B. W. (2015). Effect of dielectric packing materials on the decomposition of carbon dioxide using DBD microplasma reactor. *AIChE Journal, 61*, 898–903.
42. Chen, G., Georgieva, V., Godfroid, T., Snyders, R., & Delplancke-Pgletree, M. P. (2016). Plasma assisted catalytic decomposition of CO_2. *Applied Catalysis B: Environmental, 190*, 115–124.
43. Martini, L. M., Dilecce, G., Guella, G., Maranzana, A., Tonachini, G., & Tosi, P. (2014). Oxidaton of CH_4 by CO_2 in a dielectric barrier discharge. *Chemical Physics Letters, 593*, 55–60.
44. De Bie, C., Martens, T., van Dijk, J., Paulussen, S., Verheyde, B., Corthals, S., & Bogaerts, A. (2011). Dielectric barrier discharges used for the conversion of greenhouse gases: Modeling the plasma chemistry by fluid simulations. *Plasma Sources Science and Technology, 20*, 024008.
45. De Bie, C., van Dyke, J., & Bogaerts, A. (2015). The dominant pathways for the conversion of methane into oxygenates and syngas in an atmospheric pressure dielectric barrier discharge. *The Journal of Physical Chemistry C, 119*, 22331–22350.
46. Wang, L., Yi, Y., Wu, C., Guo, H., & Tu, X. (2017). One-step reforming of CO_2 and CH_4 to high-value liquid chemicals and fuels at room temperature by plasma-driven catalysis. *Angewandte Chemie International Edition, 56*, 13679–13683.
47. Zeng, Y., Zhu, X., Mei, D., Ashford, B., & Tu, X. (2015). Plasma-catalytic dry reforming of methane over γ-Al_2O_3 supported metal catalysts. *Catalysis Today, 256*, 80–87.
48. Nguyen, H. H., Nasonova, A., Nah, I. W., & Kim, K. S. (2015). Analysis on CO_2 reforming of CH_4 by corona discharge process for various process variables. *Journal of Industrial and Engineering Chemistry, 32*, 58–62.
49. Wang, Q., Yan, B. H., Jin, Y., & Cheng, Y. (2009). Investigation of dry reforming of methane in a dielectric barrier discharge reactor. *Plasma Chemistry and Plasma Processing, 29*, 217–228.
50. Bo, Z., Yan, J., Li, X., Chi, Y., & Cen, K. (2008). Plasma assisted dry methane reforming using gliding arc gas discharge: Effect of feed gases proportion. *International Journal of Hydrogen Energy, 33*, 5545–5553.
51. Nguyen, H. H., & Kim, K. S. (2015). Combination of plasmas and catalytic reactions for CO_2 reforming of CH_4 by dielectric barrier discharge process. *Catalysis Today, 256*, 88–95.
52. Scapinello, M., Martini, L. M., Dilecce, G., & Tosi, P. (2016). Conversion of CH_4/CO_2 by a nanosecond repetitively pulsed discharge. *Journal of Physics D: Applied Physics, 49*, 075602.
53. Kameshima, S., Tamura, K., Ishibashi, Y., & Nozaki, T. (2015). Pulsed dry methane reforming in plasma-enhanced catalytic reaction. *Catalysis Today, 256*, 67–75.
54. Abd Allah, Z., & Whitehead, J. C. (2015). Plasma-catalytic dry reforming of methane in an atmospheric pressure AC gliding arc discharge. *Catalysis. Today, 256*, 76–79.
55. Zhang, A. J., Zhu, A. M., Guo, J., Xu, Y., & Shi, C. (2010). Conversion of greenhouse gases into syngas via combined effects of discharge activation and catalysis. *Chemical Engineering Journal, 156*, 601–606.
56. Zheng, X. G., Tan, S. Y., Dong, L. C., Li, S. B., & Chen, H. M. (2015). Silica-coated $LaNiO_2$ nanoparticles for non-thermal plasma assisted dry reforming of methane: Experimental and kinetic studies. *Chemical Engineering Journal, 265*, 147–156.

57. Gallon, H. J., Tu, X., & Whitehead, J. C. (2012). Effects of reactor packing materials on H2 production by CO_2 reforming of CH_4 in a dielectric barrier discharge reactor. *Plasma Processes and Polymers, 9*, 90–97.
58. Eliasson, B., Liu, C. J., & Kogelschatz, U. (2000). Direct conversion of methane and carbon dioxide to higher hydrocarbons using catalytic dielectric-barrier discharges with zeolites. *Industrial & Engineering Chemistry Research, 39*, 1221–1227.
59. Zhang, K., Kogelschatz, U., & Eliasson, B. (2001). Conversion of greenhouse gases to synthesis gas and higher hydrocarbons. *Energy Fuels, 15*, 395–402.
60. Mahammadunnisa, S., Reddy, P. M. K., Ramaraju, B., & Subrahmanyam, C. (2013). Catalytic nonthermal plasma reactor for dry reforming of methane. *Energy & Fuels, 27*, 4441–4447.
61. Mei, D. H., Liu, S. Y., & Tu, X. (2017). CO_2 reforming with methane for syngas production using a dielectric barrier discharge plasma coupled with γ-Al_2O_3 catalysts: Process optimization through response surface methodology. *Journal of CO_2* Utilization, 21, 314–326.
62. Wang, Q., Cheng, Y., & Jin, Y. (2009). Dry reforming of methane in an atmospheric pressure plasma fluidized bed with Ni/γ-Al_2O_3 catalyst. *Catalysis Today, 148*, 275–282.
63. Sentek, J., Krawczyk, K., Mlotek, M., Kalczewska, M., Kroker, T., Kolb, T., Schenk, A., Gericke, K. H., & Schmidt-Szalowski, K. (2010). Plasma-catalytic methane conversion with carbon dioxide in dielectric barrier discharges. *Applied Catalysis B: Environmental, 94*, 19–26.
64. Kroker, T., Kolb, T., Schenk, A., Krawczyk, K., Mlotek, M., & Gericke, K. H. (2012). Catalytic conversion of simulated biogas mixtures to synthesis gas in a fluidized bed reactor supported by a DBD. *Plasma Chemistry and Plasma Processing, 32*, 565–582.
65. Krawczyk, K., Mlotek, M., Ulejczyk, B., & Schmidt-Szalowski, K. (2014). Methane conversion with carbon dioxide in plasma-catalytic system. *Fuel, 117*, 608–617.
66. Pham, M. H., Goujard, V., Tatibouet, J. M., & Batiot-Dupeyrat, C. (2011). Activation of methane and carbon dioxide in a dielectric-barrier discharge-plasma reactor to produce hydrocarbons – Influence of La_2O_3/γ-Al_2O_3 catalyst. *Catalysis Today, 171*, 67–71.
67. Goujard, V., Tatibouet, J. M., & Batiot-Dupeyrat, C. (2011). Use of a non-thermal plasma for the production of synthesis gas from biogas. *Applied Catalysis A: General, 353*, 228–235.
68. Zheng, X. G., Tan, S., Dong, L., Li, S., & Chen, H. (2009). $LaNiO_3$@SiO_2 core-shell nanoparticles for the dry reforming of CH_4 in the dielectric barrier discharge plasma. *International Journal of Hydrogen Energy, 39*, 11360–11367.
69. Zeng, Y. X., Wang, L., Wu, C. F., Wang, J. Q., Shen, B. X., & Tu, X. (2018). Low temperature reforming of biogas over K-, Mg- and Ce-promoted Ni/Al_2O_3 catalysts for the production of hydrogen rich syngas: Understanding plasma-catalytic synergy. *Applied Catalysis B: Environmental, 224*, 469–478.
70. Chung, W. C., & Chang, M. B. (2016). Review of catalysis and plasma performance on the dry reforming of CH_4 and possible synergistic effects. *Renewable and Sustainable Energy Reviews, 62*, 13–31.
71. Zheng, X. G., Tan, S. Y., Dong, L. C., Li, S. B., Chen, H. M., & Wei, S. A. (2015). Experimental and kinetic investigation of the plasma catalytic dry reforming of methane over perovskite $LaNiO_3$ nanoparticles. *Fuel Processing Technology, 137*, 250–258.
72. Montoro-Damas, A. M., Brey, J. J., Rodriguez, M. A., Gonzalez-Elipe, A. R., & Cotrino, J. (2015). Plasma reforming of methane in a tunable ferroelectric packed-bed dielectric discharge reactor. *Journal of Power Sources, 296*, 268–275.
73. Mei, D., Ashford, B., He, Y. L., & Tu, X. (2017). Plasma-catalytic reforming of biogas over supported Ni catalysts in a dielectric barrier discharge reactor: Effect of catalyst supports. *Plasma Processes and Polymers, 14*, e1600076.
74. Zeng, Y., & Tu, X. (2016). Plasma-catalytic CO_2 hydrogenation at low temperatures. *IEEE Transactions on Plasma Science, 44*, 405–411.
75. Wang, L., Yi, Y., Guo, H., & Tu, X. (2017). Atmospheric pressure and room temperature synthesis of methanol through plasma-catalytic hydrogenation of CO_2. *ACS Catalysis, 8*, 90–100.

76. De Bie, C., van Dijk, J., & Bogaerts, A. (2016). CO_2 hydrogenation in a dielectric barrier discharge plasma revealed. *The Journal of Physical Chemistry C, 120*, 25210–25224.
77. Saeidi, S., Amin, N. A. S., & Rahimpour, M. R. (2014). Hydrogenation of CO_2 to value-added products – A review and potential future developments. *Journal of CO_2* Utilization, 5, 66–81.
78. Kano, M., Satoh, G., & Iizuka, S. (2012). Reforming of carbon dioxide to methane and methanol by electric impulse low-pressure discharge with hydrogen. *Plasma Chemistry and Plasma Processing, 32*, 177–185.
79. Mora, E. Y., Sarmiento, A., & Vera, E. (2016). Alumina and quartz as dielectrics in a dielectric barrier discharges DBD system for CO_2 hydrogenation. *Journal of Physics: Conference Series, 687*, 012020.
80. Arita, K., & Iizuka, S. (2015). Production of CH_4 in a low-pressure CO_2/H_2 discharge with magnetic field. *Journal of Chemical Engineering and Materials Science, 3*, 69–77.
81. Nizio, M., Albarazi, A., Cavadias, S., Amouroux, J., Galvez, M. E., & Da Costa, P. (2016). Hybrid plasma-catalytic methanation of CO_2 at low temperature over ceria zirconia supported Ni catalysts. *International Journal of Hydrogen Energy, 41*, 11584–11592.
82. Jwa, E., Lee, S. B., Lee, H. W., & Mok, Y. S. (2013). Plasma-assisted catalytic methanation of CO and CO_2 over Ni-zeolite catalysts. *Fuel Processing Technology, 108*, 89–93.
83. Nizio, M., Benrabbah, R., Krzak, M., Debek, R., Motak, M., Cavadias, S., Galvez, M. E., & Da Costa, P. (2016). Low temperature hybrid plasma-catalytic methanation over Ni-Ce-Zr hydrotalcite-derived catalysts. *Catalysis Communications, 83*, 14–17.
84. Ponduri, S. (2016). Understanding CO_2 containing non-equilibrium plasma: Modelling and experiments. PhD Thesis, *Eindhoven: Technische Universiteit Eindhoven, Netherlands*.
85. Wang, W., Wang, S. P., Ma, X. B., & Gong, J. L. (2011). Recent advances in catalytic hydrogenation of carbon dioxide. *Chemical Society Reviews, 40*, 3703–3727.
86. Porosoff, M. D., Yan, B., & Chen, J. G. (2016). Catalytic reduction of CO_2 by H_2 for synthesis of CO, methanol and hydrocarbons: Challenges and opportunities. *Energy & Environmental Science, 9*, 62–73.
87. Liu, P., Yang, Y. X., & White, M. G. (2013). Theoretical perspective of alcohol decomposition and synthesis from CO_2 hydrogenation. *Surface Science Reports, 68*, 233–272.
88. Zou, J. J., & Liu, C. J. (2010). Utilization of carbon dioxide through nonthermal plasma approaches. *Carbon Dioxide as Chemical Feedstock*, M. Aresta (Ed.), pp 267–290. Wiley VCH.
89. Amouroux, J., Cavadias, S., & Doubla, A. (2011). Carbon dioxide reduction by non-equilibrium electrocatalysis plasma reactor. *IOP Conference Series: Materials Science and Engineering, 19*, 012005.
90. Zeng, Y. X., & Tu, X. (2017). Plasma-catalytic hydrogenation of CO_2 for the cogeneration of CO and CH_4 in a dielectric barrier discharge reactor: Effect of argon addition. *Journal of Physics D: Applied Physics, 50*, 184004.
91. Hayashi, N., Yamakawa, T., & Baba, S. (2016). Effect of additive gases on synthesis of organic compounds from carbon dioxide using non-thermal plasma produced by atmospheric surface discharges. *Vacuum, 80*, 1299–1304.
92. Eliasson, B., Kogelschatz, U., Xue, B., & Zhou, L. M. (1998). Hydrogenation of carbon dioxide to methanol with a discharge-activated catalyst. *Industrial & Engineering Chemistry Research, 37*, 3350–3357.
93. Chen, G., Silva, T., Georgieva, V., Godfroid, T., Britun, N., Snyders, R., & Delplancke-Ogletree, M. P. (2015). Simultaneous dissociation of CO_2 and H_2O to syngas in a surface-wave microwave discharge. *International Journal of Hydrogen Energy, 40*, 3789–3796.
94. Mahammadunnisa, S., Reddy, E. L., Ray, D., Subrahmanyam, C., & Whitehead, J. C. (2013). CO_2 reduction to syngas and carbon nanofibres by plasma-assisted in situ decomposition of water. *International Journal of Greenhouse Gas Control, 16*, 361–363.
95. Hoeben, W. F. L. M., van Heesch, E. J. M., Beckers, F. J. C. M., Boekhoven, W., & Pemen, A. J. M. (2015). Plasma-driven water assisted CO_2 methanation. *IEEE Transactions on Plasma Science, 43*, 1954–1958.

96. Keets, K., Morris, A., Zeitler, E., Lakkaraju, P., & Bocarsly, A. (2010). *Catalytic conversion of carbon dioxide to methanol and higher order alcohols at a photoelectrochemical interface*. Proceedings in Solar Hydrogen and Nanotechnology V. SPIE Solar Energy + Technology, San Diego (Vol. 7770, article ID: 77700R).
97. Zbudniewek, K., Goralski, J., & Rynkowski, J. (2012). Studies on TiO_2/SiO_2 and $Pd/TiO_2/SiO_2$ catalysts in photoreduction of CO_2 with H_2O to methanol. *Russian Journal of Physical Chemistry A, 86*, 2057–2062.
98. Aerts, R., Somers, W., & Bogaerts, A. (2014). CO_2 splitting in a dielectric barrier discharge plasma: A combined experimental and computational study. *ChemSusChem, 8*, 702–716.
99. Bogaerts, A., Wang, W., Berthelot, A., & Guerra, V. (2016). Modeling plasma-based CO_2 conversion: crucial role of the dissociation cross section. *Plasma Sources Science and Technology, 25*, 055016.
100. Gómez-Ramírez, A., Rico, V. J., Cotrino, J., González-Elipe, A. R., & Lambert, R. M. (2014). Low temperature production of formaldehyde from carbon dioxide and ethane by plasma-assisted catalysis in a ferroelectrically moderated dielectric barrier discharge reactor. *ACS Catalysis, 4*, 402–408.
101. Pham, M. H., Goujard, V., Tatibouët, J. M., & Batiot-Dupeyrat, C. (2011). Activation of methane and carbon dioxide in a dielectric-barrier discharge-plasma reactor to produce hydrocarbons—Influence of $La_2O_3/\gamma\text{-}Al_2O_3$ catalyst. *Catalysis Today, 171*, 67–71.
102. Frusteri, F., Bonura, G., Cannilla, C., Drago Ferrante, G., Aloise, A., Catizzone, E., Migliori, M., & Giordano, G. (2015). Stepwise tuning of metal-oxide and acid sites of CuZnZr-MFI hybrid catalysts for the direct DME synthesis by CO_2 hydrogenation. *Applied Catalysis B: Environmental, 176–177*, 522–531.
103. Witoon, T., Permsirivanich, T., Kanjanasoontorn, N., Akkaraphataworn, C., Seubsai, A., Faungnawakij, K., Warakulwit, C., Chareonpanich, M., & Limtrakul, J. (2015). Direct synthesis of dimethyl ether from CO_2 hydrogenation over $Cu–ZnO–ZrO_2$ hybrid catalysts: effects of sulfur-to-zirconia ratios. *Catalysis Science & Technology, 5*, 2347–2357.
104. Zhang, Y., Li, D., Zhang, Y., Cao, Y., Zhang, S., Wang, K., Ding, F., & Wu, J. (2014). V-modified $CuO–ZnO–ZrO_2$/HZSM-5 catalyst for efficient direct synthesis of DME from CO_2 hydrogenation. *Catalysis Communications, 55*, 49–52.
105. Centi, G., & Perathoner, S. (2009). Opportunities and prospects in the chemical recycling of carbon dioxide to fuels. *Catalysis Today, 148*, 191–205.
106. Chen, G., Georgieva, V., Godfriod, T., Snyders, R., & Delplancke-Ogletree, M. P. (2016). Plasma assisted catalytic decomposition of CO_2. *Applied Catalysis B: Environmental, 190*, 115–124.